POLISH
MARITIME
RESEARCH

in internet
www.bg.pg.gda.pl/pmr.html

POLISH MARITIME RESEARCH
No 1(51) 2007 Vol 14

CONTENTS

Editorial

POLISH MARITIME RESEARCH is a scientific journal of worldwide circulation. The journal appears as a quarterly four times a year. The first issue of it was published in September 1994. Its main aim is to present original, innovative scientific ideas and Research & Development achievements in the field of :

Engineering, **Computing & Technology**, **Mechanical Engineering**,

which could find applications in the broad domain of maritime economy. Hence there are published papers which concern methods of the designing, manufacturing and operating processes of such technical objects and devices as : ships, port equipment, ocean engineering units, underwater vehicles and equipment as well as harbour facilities, with accounting for marine environment protection.

The Editors of POLISH MARITIME RESEARCH make also efforts to present problems dealing with education of engineers and scientific and teaching personnel. As a rule, the basic papers are supplemented by information on conferences , important scientific events as well as cooperation in carrying out international scientific research projects.

Scientific Board

Investigations of influence of screw propeller operation on water flow around stern part of ship hull

Tadeusz Koronowicz
Zbigniew Krzemianowski
Institute of Fluid-Flow Machinery,
Polish Academy of Sciences
in Gdańsk

ABSTRACT

This paper presents results of measurements of velocity field in before- the - propeller flow in presence of a ship model hull of two configurations, as well as comparative calculations of velocity field on a full-scale ship. Analysis of the research results showed that input data to Biot-Savart formula should be modified in the case of calculations of propeller-induced velocities on ship hull surface.

Keywords : ship hydromechanics, propeller-induced velocities, Biot-Savart equation.

INTRODUCTION

In the 1990s in Ship Propeller Division, Institute of Fluid--Flow Machinery, Polish Academy of Sciences (IMP PAN), the computer model basin PANSHIP was elaborated. It has been aimed at simulation of ship hull model tests in ship model basin as well as relevant calculations for full-scale ship hull.

The computer model basin is a computer software system consisted of a dozen or so mutually cooperating programs [1÷6]. Crucial elements of the system are the programs capable of taking into account the influence of screw propeller operation on flow around ship hull. The software contains the programs with the use of which a change of hull resistance resulting from propeller suction action can be determined, and those by which the influence of propeller operation on velocity field in behind-the-hull flow can be taken into account.

The initial calculations performed by using the PANSHIP software have yielded generally correct results with the exception of one element : changes of hull resistance resulting from propeller operation. In ship theory such change is expressed in the form of the so-called thrust deduction **t** :

$$t = (R_T - R_o)/T = (T - R_o)/T$$

where :

R_o – resistance of hull without propeller
T – propeller thrust
R_T – resistance of hull with operating propeller (identified with propeller thrust)

The quantity **t** is usually determined during every ship model propulsion tests in model basin.

As such tests have been performed every year for many ship models, a very rich collection of experimental data in this domain has been gathered. Basing on them one can unambiguously state : the more full form of a ship the greater value of its thrust deduction **t**.

In the preliminary version of the computer model basin in question, for hulls of more full forms, greater and greater differences between calculated values of thrust deduction and those experimentally determined for the same hulls, were obtained (Fig.1). Due to prior research on flow around propeller it was possible to diagnose that **the velocities induced by whirls representing the propeller, determined by means of the Biot-Savart formula, obtained erroneous values on the hull surface**. In Fig.2 it can be observed that the more full form of a hull the smaller values of the induced velocities calculated from the original Biot-Savart formula, therefore the calculated pressures (under-pressures) on the hull surface take also smaller values.
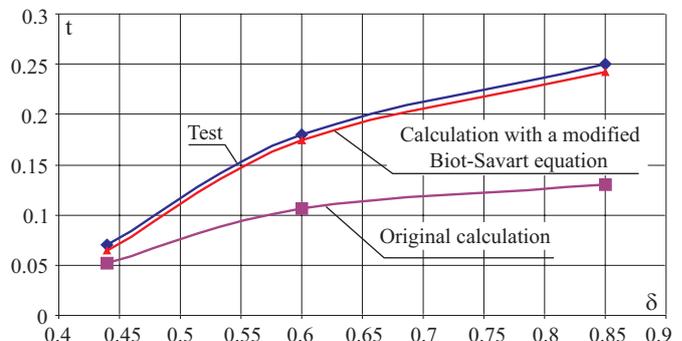
Fig. 1. A simplified diagram of the relation between the thrust deduction and hull block coefficient (in reality the relation is more complex as it depends first of all on fullness of stern part of hull) .

By analyzing the diagrams presented in Fig.2 and 3 it can be explained why such results have been obtained.
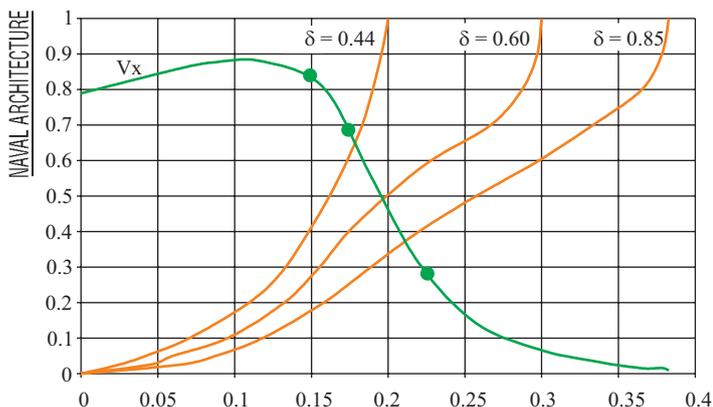
Fig. 2. Distribution of axial component of velocity in before-the-propeller flow, obtained from the original Biot-Savart formula, shown on the background of frame sections of hulls having various block coefficients .

If the velocities induced by the whirl system which represents propeller blades and propeller race, are calculated from the original Biot-Savart formula then the velocity distribution starts at the hull plane of symmetry (the point C' in Fig.3). The similar velocity distribution is presented in Fig.2, where simultaneously the frame sections of 3 ship hulls of different values of the block coefficient δ are shown. It can be observed that the greater fullness of the hull the smaller obtained values of velocities induced on its surface.
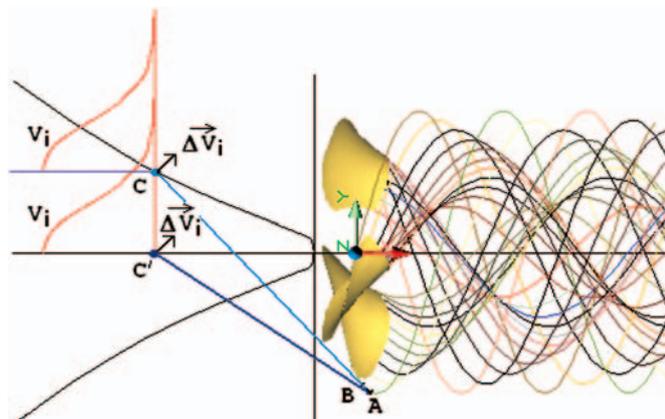
Fig. 3. Schematic presentation of the modification of data input to the Biot-Savart formula.

In the up-to-date version of the PANSHIP, was implemented a new method of calculation of induced velocities by means of Biot-Savart formula, (called the engineering method). The propeller-induced velocities were calculated in the point C' (Fig.3), but they were considered as the velocities calculated on the hull (the point C on the hull). It means that zero-value of the coordinate perpendicular to the hull plane of symmetry was put in the Biot-Savart formula. The calculation results appeared significantly better. Values of the thrust deduction obtained from calculations and those from experiments became more and more similar to each other. Obviously the described method of determination of induced velocities is only approximate, however, as revealed from practice, it yielded satisfactory results in engineering applications without any special modifications of the software.

For many years the so-modified computer software PANSHIP has been in use, and the hypothesis associated with the modification of input data for Biot-Savart formula was confirmed by comparing calculation results with experimental ones. However it was necessary to test the hypothesis by means of direct measurements of the field of the propeller - induced velocities around the hull. Such a verification is the subject of the presented work.

The model tests were performed at the Ship Hydromechanics Centre of CTO [10]. They consisted in measuring the velocity field around stern part of ship both without any propeller and with operating propeller.

The investigations were conducted on the ship model having its main particulars as follows :

Length b.p.	–	6.515 m
Breadth	–	0.977 m
Draught	–	0.376 m
Model scale	–	$\lambda = 33$

The hull frame sections are shown in Fig.4.

Stern   Bow
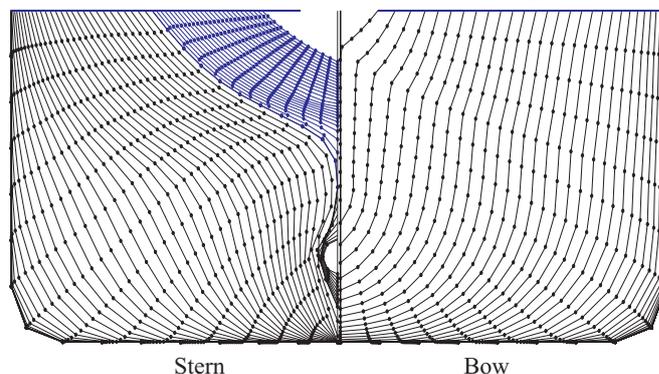
Fig. 4. Image of the panels projected on the model frame sections .

The applied measuring instrument (the measuring sounder fitted with the single five-hole spherical head PKN(5+4)/8/1) made it possible to measure the velocity components Vx, Vy, Vz in the hull-fixed rectangular coordinate frame :

➢ x – component : along ship axis of symmetry and hull motion direction
➢ y – component : perpendicular to the hull plane of symmetry
➢ z – component : perpendicular to the hull water plane.

The measurement space was located at the port side of the hull.

Distance of propeller working plane from aft perpendicular – Xp = 124 mm

Distance of propeller axis from plane of symmetry – Yp = 0.0 mm

Distance of propeller axis from base plane – Zp = 109.1 mm.

The measurement plane was located $\Delta X = 157$ mm fore from the propeller working plane.

EXPERIMENTAL TESTS

The measurements were performed at one value of the ship model velocity $V_M = 1.75$ m/s and four values of rotational speed of the propeller model. The first value of rotational speed was determined for zero-value of propeller thrust. It was assumed that this was the rotational speed at which propeller-induced velocities on the hull were of negligibly small values, hence the velocity measurements could be considered equivalent to the tests on the hull without propeller. The value of $n_o = 7.3$ rps resulted from the tests (during the tests values of both propeller - induced thrust and torque as well as hull resistance were measured).

The next three values of rotational speed were so selected as to obtain only significantly large values of propeller - model--induced velocities. With taking into consideration the working

range of the measuring dynamometer the following three values of rotational speed were selected :

$$n_1 = 25 \ 1/s \ ; \ n_2 = 30 \ 1/s$$
$$n_3 = 35 \ 1/s.$$

At the obtained values of rotational speeds the values of propeller thrust were many times greater than that of hull resistance at the speed $V_M = 1.75$ m/s.

The measurements were conducted along two measurement lines perpendicular to the longitudinal plane of symmetry of the hull, **XZ**, placed by $\Delta X = 157$ mm apart from the propeller working plane. **The first line is placed at the height of propeller rotation axis, the other - 50 mm above the mentioned axis**.

The first measurement point was selected as close to the hull surface as possible, and the successive points were placed at every **20 mm** up to the distance assumed negligible from the point of view of propeller – induced velocities.

The selected measurement results are presented in Fig. 5÷8 whereas the complete set of them - in CTO's report [10], and their graphical representation - in the IMP PAN report [11]. Values of the velocity components V_x, V_y, V_z and of the total velocity V_c can be found there. During all the tests the ship model speed V_M was kept equal to 1.75 m/s.

In Fig.5 are presented the measurement results at the rotational speed n = 7.3 1/s corresponding with zero-value of propeller model thrust. Hence it can be assumed that the velocities shown in Fig. 5 correspond with those around the hull without propeller. They have been taken as the reference point for determining the velocities induced by working propeller model.
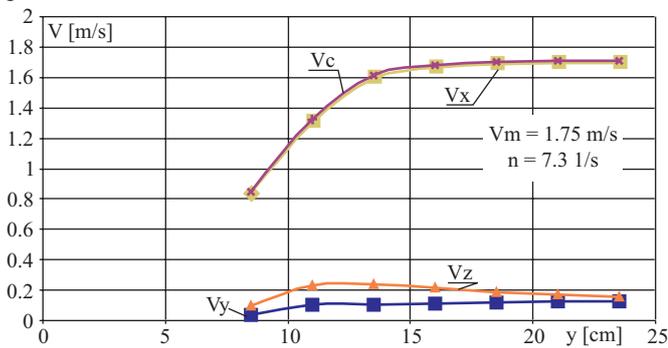
Fig. 5. Velocity components along the measurement line located at the height of the propeller axis, for n = 7.3 1/s (thrust of zero-value) .

In Fig.6, 7 and 8 are presented results of the measurements at higher rotational speeds of propeller model, for which induced velocities should already show significant values. In Fig.9 it can be observed in which way values of the axial component (marked x) change along with rotational speed changing.
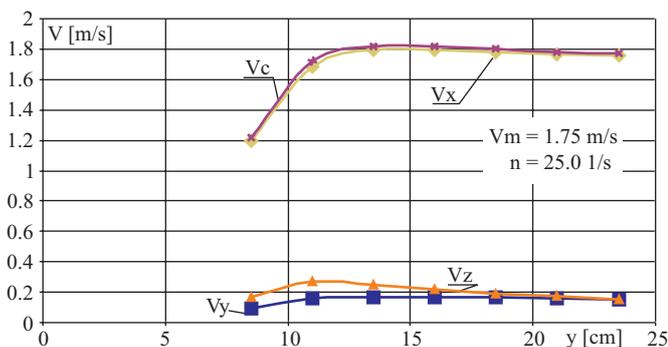
Fig. 6. Velocity components along the measurement line located at the height of the propeller axis, for n = 25 1/s .
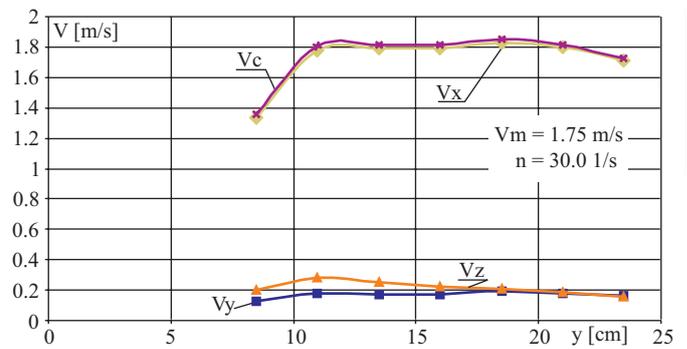
Fig. 7. Velocity components along the measurement line located at the height of the propeller axis, for n = 30 1/s .
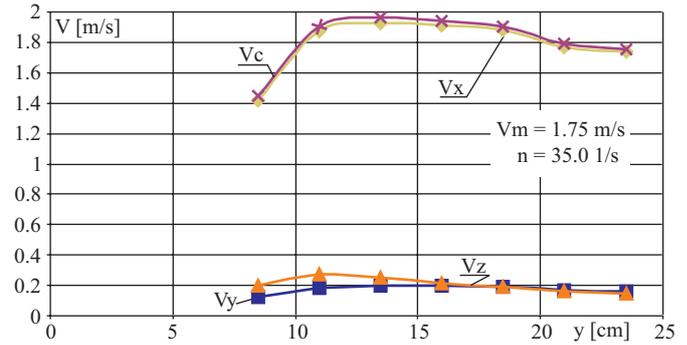
Fig. 8. Velocity components along the measurement line located at the height of the propeller axis, for n = 35 1/s .
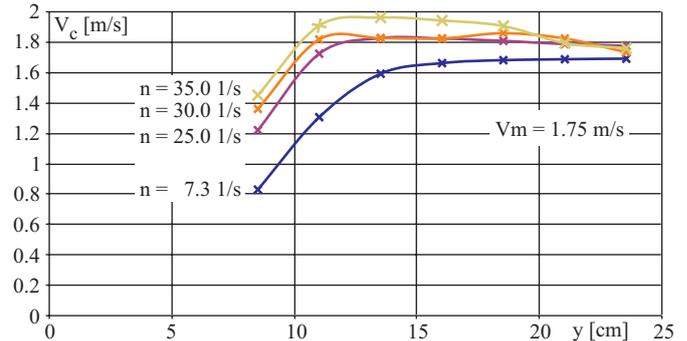
Fig. 9. Modules of velocities along the measurement line located at the height of the propeller axis, for various values of propeller rotational speed .

In Fig.10 are presented the differences between the velocities obtained at high values of rotational speed and the velocity corresponding with the thrust of zero-value. They should correspond with the propeller-induced velocities but the character of the changes indicates that the influence of viscosity on the velocity distribution is significant (induced velocities make velocity distribution in the boundary layer changing).
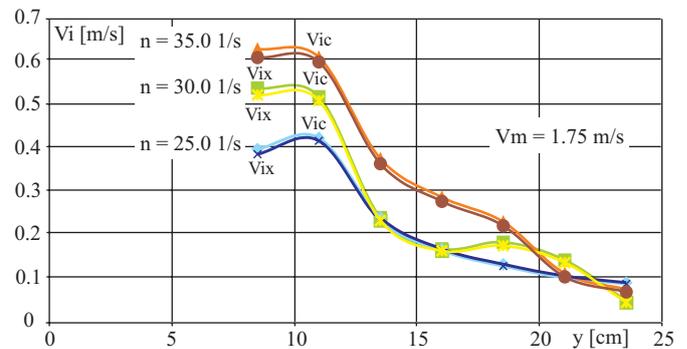
Fig. 10. Axial component and module of propeller-induced velocity along the measurement line located at the height of the propeller shaft axis .

Similar measurements were performed at the measurement line located in the same plane but at the height above the propeller rotation axis by 50 mm. For the measurements only the final diagram of the propeller induced velocities is presented.
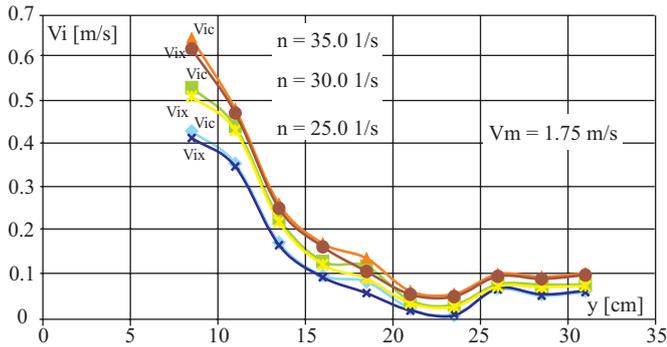
Fig.11. Axial component and module of propeller-induced velocity along the measurement line located at the height above the propeller shaft axis by 50 mm .

Analyzing the above presented results of the investigations, especially those of Fig. 10 and 11, one can state that the share of propeller-induced velocities in the total velocity is significant (intentionally the values of propeller rotational speed considerably exceeded the own propulsion point of the model, which, for the velocity V=1.75 m/s, approximately corresponded with the rotational speed of 13 rps).

To confirm hull influence on calculation results of propeller-induced velocities it should be necessary to perform measurements in two frame cross-sections located nearby to each other but having significantly different transverse offsets (breadth). Unfortunately, for many years the ship models designed and tested have been characterized by slender stern forms. For this reason the second cross-section was chosen beyond the stern. In order to maintain the distance between the working plane and measurement cross-section the way of fastening the propeller shaft was changed. The stern part of the hull was modified by extending the stern tube in such a way as to get the measurement cross-section placed beyond the stern and the propeller model placed at the same distance as in the case of basic tests (Fig.12). The tests on such hull version were called the tests on the Ship 2.
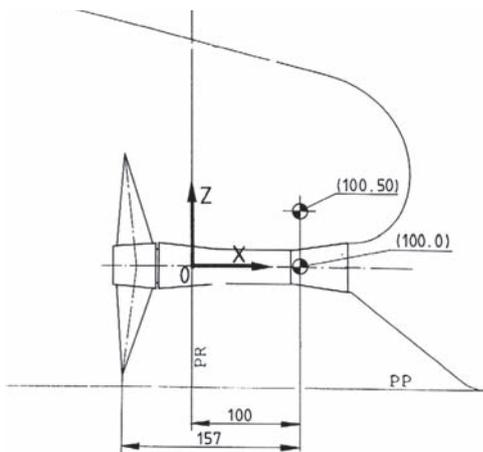
*Fig. 12. Location of measurement lines on the ship model with the modified stern. **PP** - Base plane, **PR** - Aft perpendicular .*

The measurements were performed at the same ship model speed V_M = 1.75 m/s and four values of rotational speed of propeller model, in the same way as in the first cycle of investigations. Their results for the sounder located at the height of the shaft axis are presented in Fig.13. (The comprehensive set

of the results from the measurements and calculations can be found in the CTO report [10] and IMP PAN report [11]).
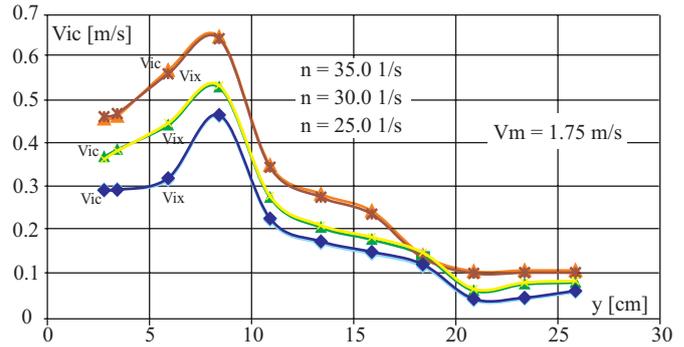
Fig. 13. Axial component and module of propeller-induced velocity measured at the height of the propeller shaft axis of the ship model with the modified stern, at the distance of 157 mm before the propeller .

Comparing, with each other, the measurement results for both versions of propeller fastening (Fig.14) one can state that the curves are mutually shifted. The difference is approximately equal to the difference of hull breadth and propeller shaft in the places where the measurements have been performed in both versions of the tests.
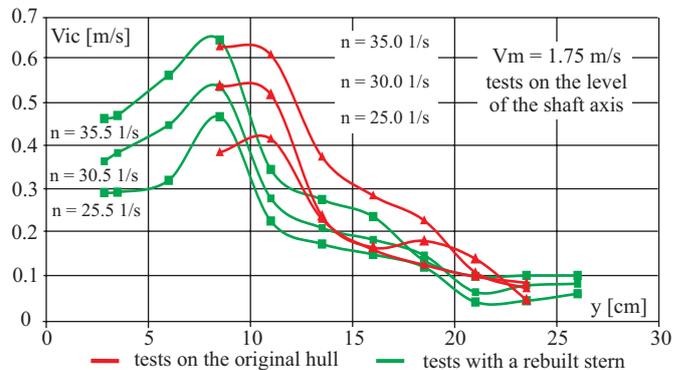
Fig. 14. Comparison of induced velocities obtained from the tests on the models with the original stern and modified one .

Therefore the experimental tests fully confirmed the put hypothesis as follows :

Calculations of the velocities around ship hull, induced by whirl systems representing the propeller itself and propeller race, make it necessary to modify input data to Biot-Savart formula, and as a result of the tests in question the proposed modification of the input data has been proved correct.

TESTS ON FULL-SCALE SHIP

The scientific aim of the presented investigations is to improve the algorithm applied in the software for calculating 3D velocity field in the stern part of full-scale ship with taking into account propeller operation [7]. Therefore an important element of the investigations is to verify such field on a full-scale ship.

It is very hard to achieve reliable results from full-scale measurements of such field. In the subject-matter literature are known results of the measurements performed, both in model - and full-scale, on the hull of HSVA tanker ship, realized under the auspices of the model basin in Hamburg.

The measurements of the velocity field before the propeller working on the full-scale ship were carried out through a window panel fitted in the stern part of the hull. They were conducted with the use of a laser anemometer but only respective to the axial component of total velocity (i.e. with taking into account propeller-induced velocities) The measurement

results are presented in the form of diagrams of isotachs, and only in the range covered by laser beam (Fig.15). The measurements were performed at the distance X = 0.21D from aft perpendicular. The broken line denotes the propeller circle of the diameter D = 6.1 m.

(Hamburg Test Case) : full scale total axial velocity distribution; Vs = 9.26 m/s
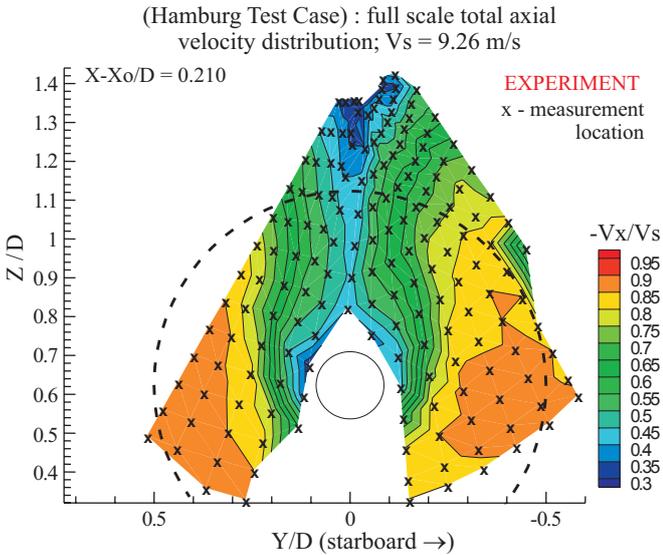
Fig.15. *Results of the measurements of axial velocity component, performed on the ship with operating propeller .*

And, in Fig.16 are presented the calculation results obtained from the modified PANSHIP software, also concerning only the axial component of velocity in the same cross-section before the propeller.

Axial component of effective velocity field behind the hull, V_X/V_S
Effective wake fraction $w_n = 0.2249[-]$
Effective wake fraction $w_{n1} = 0.2273[-]$
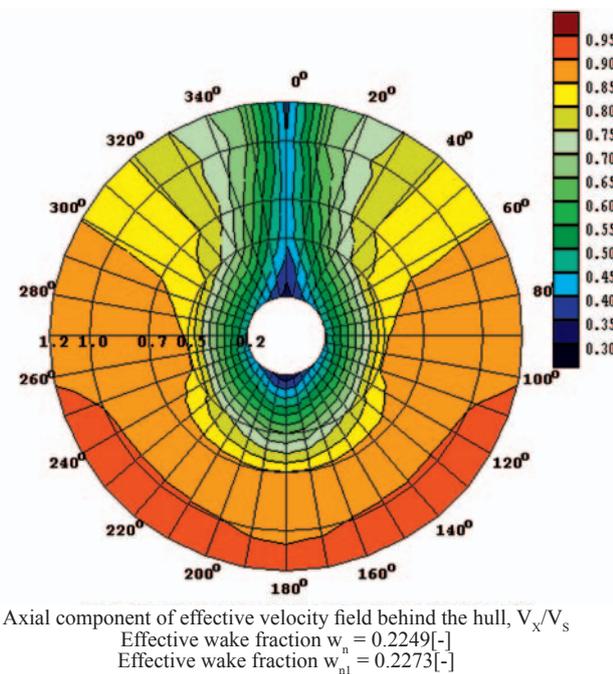
Fig. 16. *Results of the measurements of axial velocity component, performed on the ship with operating propeller .*

On the basis of analysis of the achieved results of calculations, performed on the background of measurement results (compare Fig.15 and Fig.16), a qualitative similarity of both fields can be stated. Quantitative comparison can be more clearly presented in another form. In Fig.17, 18 and 19 the same results are shown in the form of diagrams of velocity at a given radius. To this end three radiuses : r/R = 1.0, 0.7 and 0.5 were selected.

If only accuracy of the measurements on the full-scale ship are taken into consideration (the curves presented in the figures should be symmetrical respective to the ship plane of symmetry) then the so-presented results are found astonishingly similar for the radiuses r/R = 1.0, and especially r/R = 0.7). It means that the PANSHIP software correctly determines the velocity field in the behind- the- hull flow and correctly expresses the velocity field induced by the propeller. In the diagrams are presented total velocity values which are formed along a considerable length of hull stern part at a significant share of propeller-induced velocities. It confirms that the PANSHIP can be successfully applied to the scaling of velocity fields on full-scale ship [7].
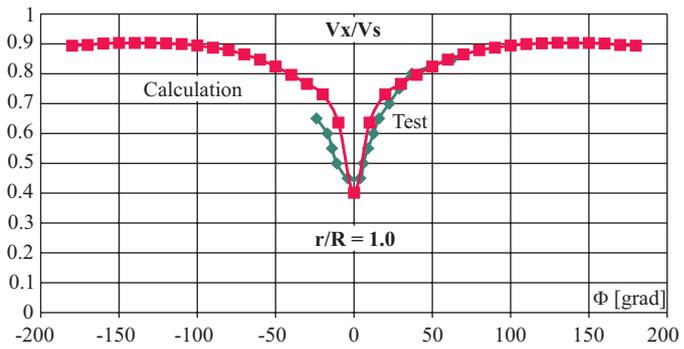
Fig. 17. *Comparison of the axial component of before-the-propeller velocity at the radius r/R = 1.0, obtained from measurements and calculations for the full-scale ship, respectively .*
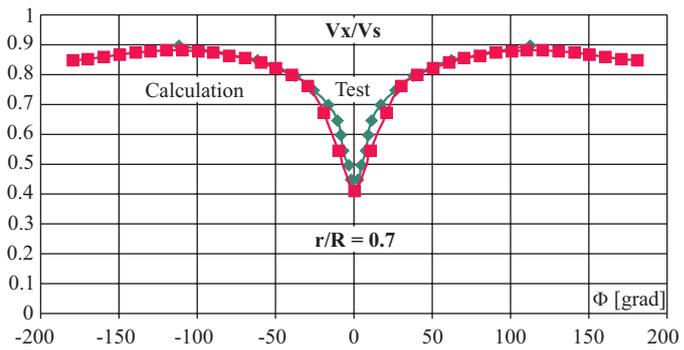
Fig. 18. *Comparison of the axial component of before- the - propeller velocity at the radius r/R = 0.7, obtained from measurements and calculations for the full-scale ship, respectively .*
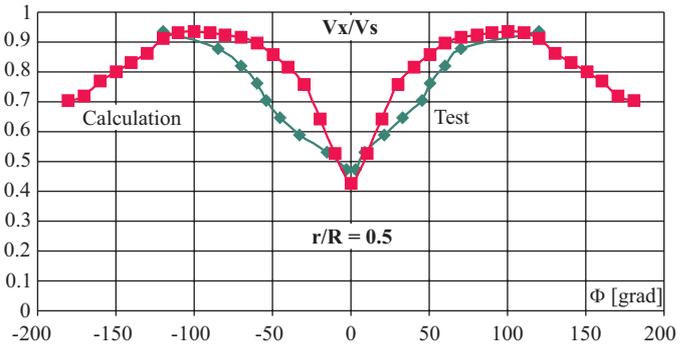
Fig. 19. *Comparison of the axial component of before- the - propeller velocity at the radius r/R = 0.5, obtained from measurements and calculations for the full-scale ship, respectively .*

FINAL REMARKS

❍ It can be concluded that the obtained experimental tests fully confirmed the proposed hypothesis :
Calculations of velocities around the ship, induced by whirl systems representing the propeller itself and propeller race require input data to Biot-Savart formula to be modified.

○ The proved hypothesis can be considered as a kind of discovery in fluid mechanics (in handbooks on hydromechanics and subject-matter literature no mention on that theme can be found)

○ However further theoretical research aimed at building a correct form of Biot-Savart formula in multiply connected space, is necessary

○ The proposed modification of the way of calculations of velocities induced around ship hull can be tentatively implemented in engineering practice as an effective approximation.

NOMENCLATURE

B – hull breadth
D – propeller diameter
L – hull length
n – number of propeller revolutions per second
r – radius of cylindrical cross-section around propeller axis
R – propeller radius
R_o – hull resistance
R_T – resistance of hull with operating propeller
t – thrust deduction
T – propeller thrust, also hull draught
V_M – model speed
V_S – ship speed
V_c – total velocity $\sqrt{(V_M + V_x)^2 + V_y^2 + V_z^2}$
V_i – induced velocity
V_{ic} – total induced velocity $\sqrt{V_x^2 + V_y^2 + V_z^2}$
Vx, Vy, Vz – velocity components
X_p, y_p, z_p – coordinates of propeller axis location
y – distance of measurement points from hull plane of symmetry
δ – hull block coefficient
Δ – hull buoyancy
ΔV_i – velocity induced by whirl filament's element
λ – model scale

BIBLIOGRAPHY

1. Bugalski T., Koronowicz T., Szantyr J., Waberska G.: *Computer software for determining flow around the ship together with wave system* (in Polish). Proceedings of 10th Symposium on ship hydromechanics, Gdańsk. 1993

2. Bugalski T., Koronowicz T., Szantyr J., Waberska G.: *Computer system for calculation of flow, resistance and propulsion of a ship*; Paper presented at CADMO'94. Southampton UK, 1994

3. Bugalski T., Koronowicz T., Szantyr J., Waberska G.: *A metod for calculation of flow around the hull of a ship moving in calm water with constant velocity"*; Marine Technology Transactions, vol. 5. 1994

4. Koronowicz T., Tuszkowska T., Bugalski T., Grabowska K.: *The influence of propeller operation on the pressure field on the hull and around it;* Proceedings of 12th International Conference on Hydrodynamics in Ship Design, HYDRONAV'97, Szklarska Poręba, September 1997

5. Koronowicz T., Szantyr J., Bugalski T.: *Theoretical model for determining the pressure field resulting from hull flow and operation of the marine propeller;* Polish Maritime Research, September 1997

6. Koronowicz T., Tuszkowska T., Waberska G.: *Computer software system for determining the pressure field resulting from hull flow and operation of the marine propeller;* Polish Maritime Research, December 1997

7. Koronowicz T.: *A computer method for prediction of the velocity field behind a full-scale ship hull*, Polish Maritime Research No 1/2003, vol. 10

8. Koronowicz T., Tuszkowska T., Waberska G.: *Modernization of the calculation model applied to the computer software PANSHIP* (in Polish). IMP PAN Report

9. Koronowicz T., Tuszkowska T., Waberska G., Kaniecki M., Krzemianowski Z.: *Analysis of preliminary results of tests* (in Polish). Report no. 4643/04. IMP PAN

10. Jaworski S.: *Results of measurements of velocity field before the propeller which operates on ship model and axially symmetrical bodies* (in Polish). Technical report no. RH-2004/T-149, Ship Design & Research Centre

11. Koronowicz T., Tuszkowska T., Waberska G., Kaniecki M., Krzemianowski Z. : *Analysis of results of velocity field tests on the model 1* (in Polish). Report no. 4864/04, IMP PAN (Institute of Fluid-Flow Machinery, Polish Academy of Sciences in Gdańsk)

12. Koronowicz T., Koronowicz J., Niewiadomski J., Bunikowski J., Huk G.: *Measurements of propeller-induced velocity field around an axially symmetrical body in cavitation tunnel* (in Polish). *Report no. 5065/05*, IMP PAN

13. Koronowicz T., Tuszkowska T., Wawerska G., Kaniecki M., Krzemianowski Z., Koronowicz J., Chaja P., Bednarek A.: *Analysis of results of tests of an axially symmetrical body in model basin* (in Polish). Report no. 5104/05, IMP PAN

14. Koronowicz T., Bugalski T., : *Analysis of results of tests of a ship* (in Polish), Report no. 5220/05, IMP PAN

15. Koronowicz T., Krzemianowski Z.: *Experimental research on propeller influence on flow around ship hull* (in Polish). Materials of MWK-2005, vol. III, Waplewo 17-20 May 2005

16. Koronowicz T., Krzemianowski Z.: *The numerical and experimental tests of the work of a screw propeller on the flow around the hull on a ship*, Materials of the International Conference HYDRONAV'05, Gdańsk-Ostróda

CONTACT WITH THE AUTHORS

Prof. Tadeusz Koronowicz
Zbigniew Krzemianowski, D.Sc., Eng.
Institute of Fluid-Flow Machinery,
Polish Academy of Sciences
Fiszera 14
80-952 Gdańsk, POLAND
e-mail : ttk@interecho.com

*C*onference

REGIONAL GROUP of the Section on Exploitation Foundations

On 25 May 2006 the Regional Group of the Section on Exploitation Foundations, Machine Building Committee, Polish Academy of Sciences (PAS), held its successive scientific seminar organized by Faculty of Engineering Sciences , Warmia - Mazury University in Olsztyn.

Scientific workers of the Faculty presented the following papers :

➡ *A method for improving operation processes of track engine* – by B. Kolator

➡ *Application of Exsys Covrid to maintenance of machines* – by K. Ligier and A. Rychlik

➡ *A system for maintaining the machines in tero-technological approach* – by P. Mikołajczak

After discussion and replies from the side of the authors to questions directed to them, the organizers presented scientific laboratories of the Faculty.

Miscellanea

The books *Ship Turbine Power Plants: Fundamentals of Thermodynamical Cycles* and *Introduction to the Theory of Marine Turbines* by Krzysztof Kosowski form the first two volumes of a series of four monographs on marine turbine power plants. They are meant for mechanical engineers and for graduate students of technical universities, as well as marine and naval academies. They were initially elaborated as part of the EuroMTEC program for the module *Advanced Ship Propulsion and Equipment*, and have now been remarkably developed and noticeably extended. When writing them the author made use of some of the most outstanding works on the subject and to take into account his experiences from work at university. Fundamentals of power plant cycles and principles of turbine operation were laid out using renowned books ranging from the first works of A. Stodola published 100 years ago to the latest scientific papers and information given by major turbine producers.
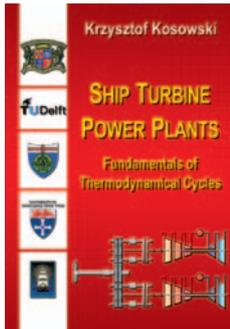
Ship Turbine Power Plants: Fundamentals of Thermodynamical Cycles
This book deals with thermodynamical cycles of steam and gas turbines, and turbine power plant arrangements.

Chapter 1: Fundamental Principles of Thermodynamics
Chapter 2: Steam Turbine Cycles
Chapter 3: Gas Turbine Cycles
Chapter 4: Combined Turbine Cycles

(ISBN: 83-922007-2-1, Published by: Foundation for the Promotion of Maritime Industry, Gdańsk, 2005, 280 pages, hardback, full colour)
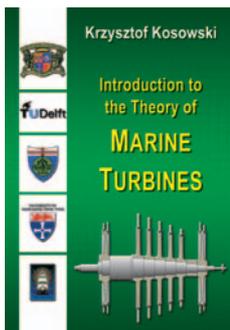
Introduction to the Theory of Marine Turbines
This book deals with the fundamental aspects of axial turbine theory.

Chapter 1: Review of Gas Dynamics
Chapter 2: Axial Stage Theory
Chapter 3: Stage Internal Losses
Chapter 4: Efficiency Characteristics
Chapter 5: Calculations of Flow in Turbine Stages
Chapter 6: Multi-stage Turbines

(ISBN: 83-922007-3-X, Published by: Foundation for the Promotion of Maritime Industry, Gdańsk, 2005, 261 pages, hardback, full colour)

The books have earned high appreciation of the reviewers:

„The author deals not only with turbine theory, but also with a wide range of aspects connected with strength, operation, technology and dynamics. [...] The discussed problems are presented in a clear and concise way [...] and the book meets all standards of an academic handbook."

„The handbook contains not only a classical approach to the principles of turbomachinery, but also presents state-of--the-art design methods and results of recent research."

„The form of presentation of the material and the collected examples deserve admiration [...], while the text and figures are excellently chosen."

About the author

Krzysztof Kosowski is an Associate Professor at the Chair of Ship Automation and Turbine Propulsion, Gdańsk University of Technology. His scope of interest includes selected problems in the theory, design and construction of steam and gas turbines. He has delivered lectures on turbine theory, turbines and compressors, power plants, fluid flow mechanics, thermodynamics, turbine design, nuclear turbines and rotating machinery.

His scientific activity is focused on theoretical and experimental research into turbine stages, dynamics of rotor systems, active control of flows and mechanical vibrations, as well as three-dimensional flow calculations in turbomachinery, optimisation of turbine flow parts and thermodynamical cycles.

Analysis of hull resistance
of pushed barges in shallow water

Tomasz Tabaczek
Jan Kulczyk
Maciej Zawiślak
Wrocław University of Technology

ABSTRACT

These authors performed a set of numerical calculations of water flow around pushed barges differing to each other by bow forms. The calculations were executed by means of FLUENT computer software. Turbulent free-surface flow of viscous liquid was considered. In this paper the calculated values of barge hull resistance split into bow, cylindrical and stern part components, have been compared and presented.

Keywords : inland waterways ship, hull resistance

INTRODUCTION

The barges operating in push-train mode are characterized by great values of the hull block coefficients ($C_B > 0.85$), that ensures achieving large values of their displacement at assumed main dimensions. On the other hand, to decrease their building costs, usually is applied a simplified bow form consisted of practically developable surfaces divided by chine lines, thus relatively simple in building. Such approach is a rational and economical compromise since service speed of ships on inland waterways is of the order of $10 - 15$ km/h.

An inspiration to undertake the research on hull resistance of inland navigation cargo ships has been given by the information coming from an inland navigation ship owner that the fuel consumption on a given shipping route differs significantly in the case of pushed barges differing to each other first of all by their bow forms. These authors decided to investigate which bow forms of pushed barges ensure obtaining the smallest hull resistance values. To this end several characteristic bow forms were selected [1]. Each of the selected characteristic forms has been adjusted to a barge having the main dimensions : $L_C \times B \times T = 48.75 \times 9.0 \times 1.7$ m, under the assumption that the bow length from the end of the cylindrical midship body up to the bow transom plane is equal to $L_E = 8.0$ m. Next, series of calculations of the flow around the push-trains consisted of two barges connected to each other by their stern parts, were performed. The calculations were executed by means of the FLUENT commercial computer software which makes it possible to take into consideration all factors of crucial influence on ship resistance, i.e. viscosity of water, turbulence of flow, as well as wave system on water free-surface around the ship.

Quality of the calculation results of free-surface water flow around inland navigation ships in shallow water, has been assessed during the previous research investigations carried out by these authors [2 , 3]. In view of a limited performance of the computers being at the authors' disposal most of the computations was performed for the hulls in a reduced scale. As a rule the same scale has been applied as in the case of model testing in a towing tank. A direct comparison of the results of the calculations with those from model tests has confirmed that the applied software is useful in calculating hull resistance and determining wave profile on the ship side.

HULL FORMS
OF THE CONSIDERED BARGES

The calculations of water flow around hulls of the barges were performed for 11 trains of barges fitted with bows of the following forms (Fig.1) : EIIB, EIIBM, EIIBV2, EIIBH, ELI, ELIM, WALE, WALC, B, B3 and HEL. The first four constitute a group of similar forms. They have been elaborated on the basis of the hull form of the EUROPA IIb pushed barge popular on the West - European waterways. They differ to each other by the shape of longitudinal cross-section contour in the plane of symmetry. For the four barges similar results were achieved. The hull form of ELI barge has been elaborated on the basis of an elliptical bow (Ellipsenbug) proposed by Nussbaum [4]. The ELIM form is a simplified version of the ELI form. Rounded segments of frame sections have been replaced by straight-line segments inclined by the angle of 45°. As a result, the surface between the bottom and side of hull has become a developable surface. The WALE and WALC forms have vertical sides and are of the simplest geometry. They differ to each other only by a shape of water-planes which are elliptical in the first case, and in the other − circular segments tangent to ship sides. The B and B3 bow forms have been designed by the team working on the project. The form B ensures obtaining a high block coefficient value of the bow. Owing to the flat bottom it is possible to make the barge cubicoid hold much longer. The other bow form is more fine – it has a more inclined stem and higher elevated line of the side chine. The HEL bow form has been designed by these authors. Side surface of the bow
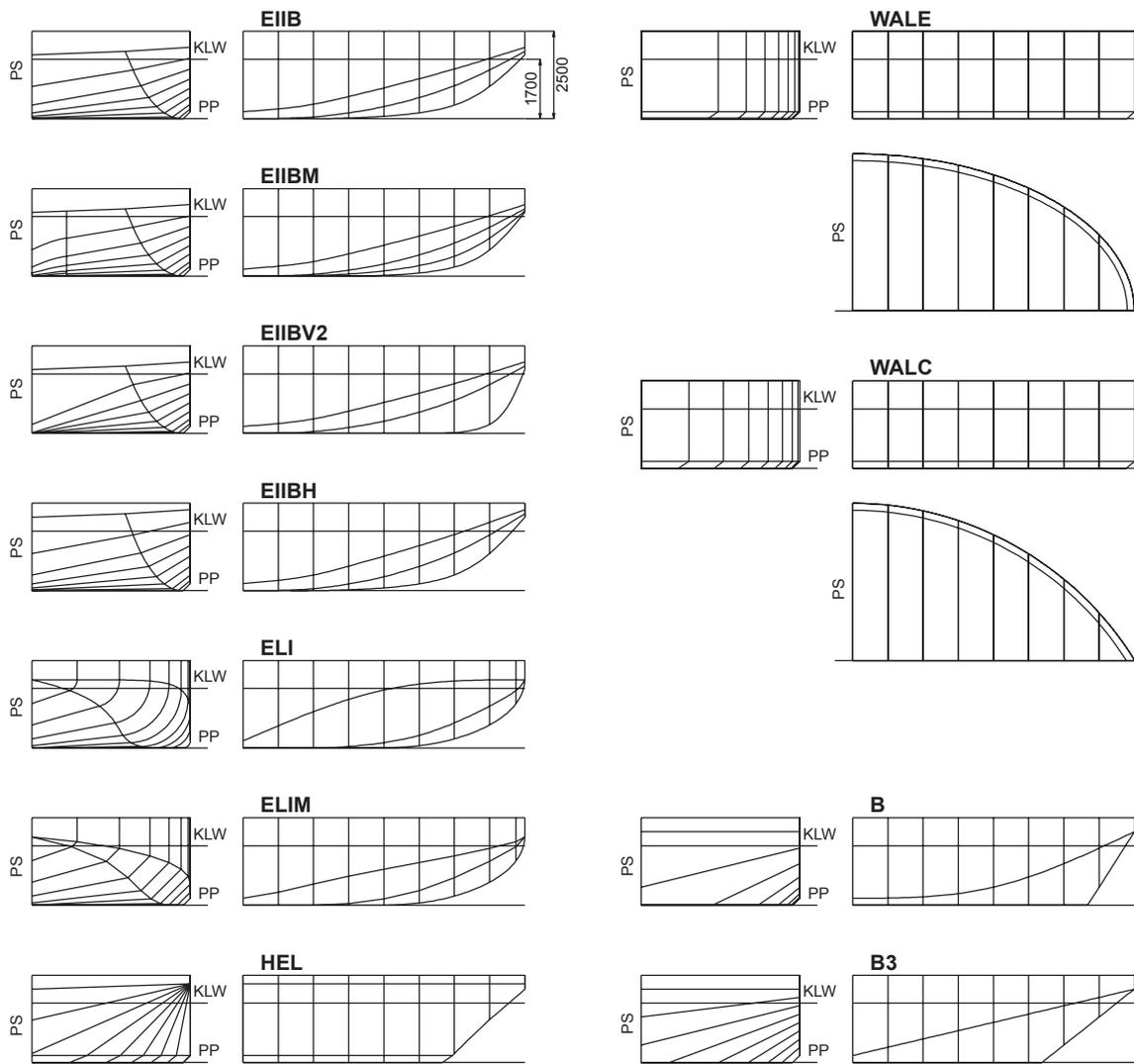
*Fig. 1. Hull forms of the considered barges. **PS** - Plane of symmetry, **PP** - Base Plane, **KLW** - Design waterline .*

is a fragment of a regular helicoid with its axis located in the plane of hull side. This shape was assumed to jostle water aside like the WALC form and simultaneously to integrate a broad deck and bow transom like in the case of the EIIB bow form. In the below presented table, are given values of the block coefficient of hull and that of bow which has been defined as follows : $C_{BE} = V_E/(L_E \times B \times T)$.

The authors have intended to check if any unambiguous relation between values of the above mentioned coefficients and hull resistance, takes place.

Bow	C_B	C_{BE}
EIIB	0.952	0.705
EIIBM	0.952	0.709
EIIBV2	0.956	0.742
EIIBH	0.951	0.675
ELI	0.950	0.695
ELIM	0.949	0.699
WALE	0.962	0.782
WALC	0.949	0.700
B	0.974	0.823
B3	0.952	0.663
HEL	0.939	0.589

The calculations were performed for the train of two barges connected to each other by their stern parts. To elaborate grids for numerical calculations the assumption was made that the stern form of a single barge influences train's resistance to the same degree, irrespective of an applied bow version. For this reason the aft bottom undercut was not modelled and the cylindrical parts of both barges were made longer and joined together in the aft transom plane.

The identical flat bilge form of 200 mm in height, was applied to all the barges, except of those having ELI bow form, where the cylindrical bilge form of 200 mm radius was used.

CALCULATION CONDITIONS

The flow calculations were performed for two values of water depth: 2.0 m and 3.4 m. The first of them models the conditions of very shallow water (h/T = 1.18). In the case of canalised rivers such conditions appear only in certain places – along short sections of a waterway. The other water depth (h = 3.4 m) models shallow water conditions, which is more real-istic for average service conditions on the domestic waterways.

In both the cases the calculations were carried out for the ship speed equal to 2.48 m/s (8.93 km/h). i.e. at the Froude number $Fn_h = 0.56$ in a more shallower water, and $Fn_h = 0.43$ in a deeper water. At such speed a significant sagging of the ship should be taken into account, especially at the water depth equal to 2.0 m. However the taking of sagging into account in calculations is associated with a change of location of bound-

aries of computation area and a significant increase of time of computations. The authors have assumed that the neglecting of sagging introduces the same errors to resistance values of all the considered hull forms. Hence the differences in calculated resistance values would maintain the same, and to compare directly the bow forms would be possible.

For the calculations performed within the frame of this research work the authors made use of the same principles of building the computational grids and controlling calculation runs as those used in the previous research work [3].

All the calculations were performed in the model-scale of 1:14. The computational grid covered the rectangular area extending up to 41.25 m ahead the bow and behind the stern, and 45.5 m overboard. The grid mesh was so designed as to ensure precise modelling the hull form and the flow around hull surface. As a rule a regular grid consisted of cubicoid elements was applied, but irregular one – only locally. For the reason of a limited computer performance the number of elements did not exceed 200 000.

In the FLUENT software the problem in question was defined as non-stationary one. The equations were integrated till reaching a stationary state. The applied time-step of 0.01s ensured reaching the convergence of calculations after 30 000 steps. To model the turbulence phenomenon the model RNG k-ε was selected. A single run of calculations took 48 h on average.

RESULTS

In contrast to the experimental methods (towing tank model tests) the application of the numerical computation method to fluid mechanics (CFD) makes it possible to split hull resistance into the components resulting from normal stresses (pressure) and tangential stresses (liquid viscosity). It also makes it

possible to easily determine forces acting on various parts of the hull. In order to analyse a contribution of particular hull segments in total hull resistance the authors split the entire hull surface into three parts :

❖ the bow (from the bow transom plane of fore barge to the cylindrical midship body)
❖ the cylindrical midship body (precisely – joined midship bodies of both fore and aft barges), and
❖ the stern (from the cylindrical midship body of aft barge to the bow transom plane of aft barge) (Fig.2).
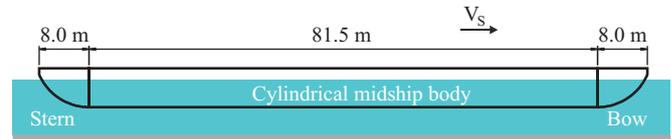
Fig. 2. The train of two barges split into three parts for resistance analysis purposes

The below presented values of hull resistance, calculated by means of the FLUENT software for free-surface flow conditions, take into account hydrostatic pressure.

In further considerations it was assumed that hull resistance is a force acting in the direction opposite to ship speed vector (i.e. aft). A negative value of stern resistance means that the resultant force acting onto the stern is directed fore. The greater the force the smaller the total hull resistance. In Fig.3 and 4 the bow forms are ranked in a sequence resulting from increasing value of total resistance.

In design and service practice, quality of a pushed barge hull form is assessed by using the unit resistance values, i. e. those taken per unit buoyancy or volume of underwater part of ship's hull. The unit resistance values are compared in Fig. 5.
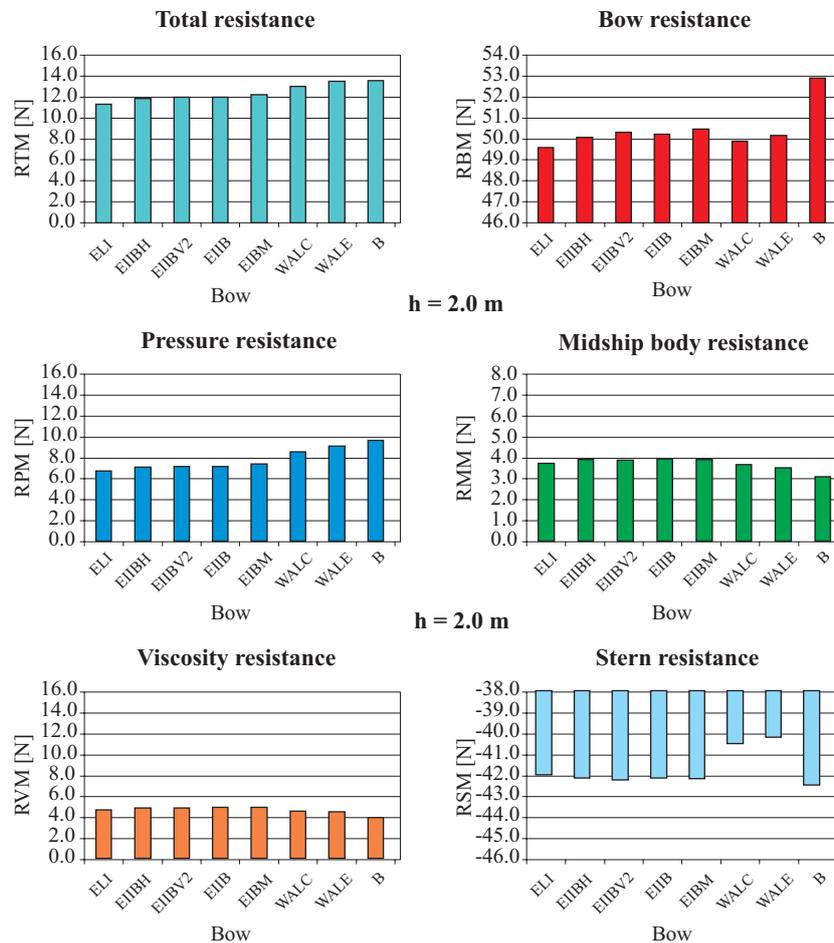
Fig. 3. Resistance of the two-barge-train model at the water depth of 2.0m .

Total resistance

Bow resistance

h = 3.4 m

Pressure resistance

Midship body resistance

h = 3.4 m

Viscosity resistance

Stern resistance

Fig. 4. Resistance of the two-barge-train model at the water depth of 3.4 m .

Unitary resistance h = 2.0 m
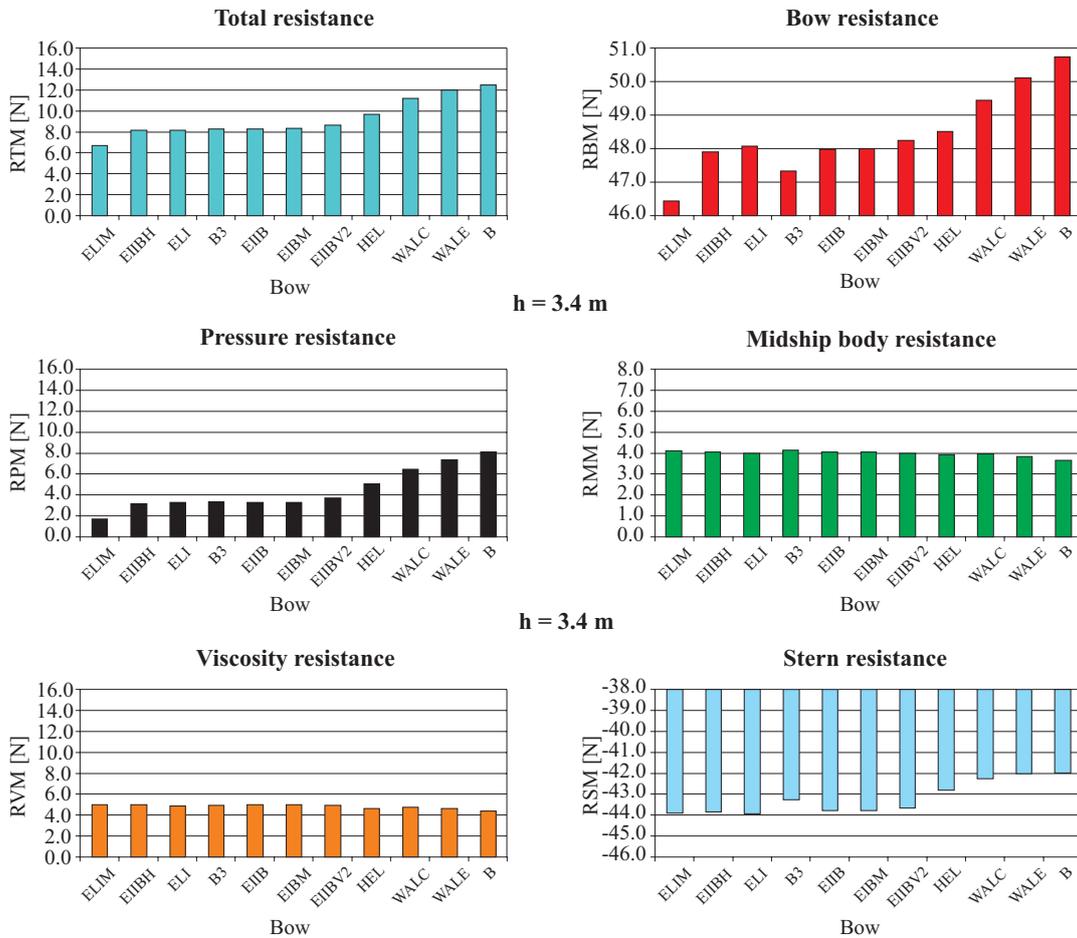
Unitary resistance h = 3.4 m
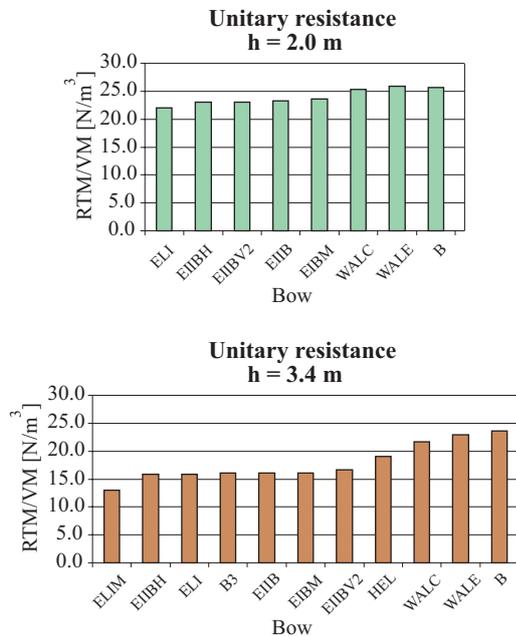
Fig. 5. The unit resistance values of the two-barge-train model .

SUMMARY

○ Onto the hulls jostling water aside (HEL, B, WALC, WALE) is exerted a greater pressure resistance and smaller viscosity resistance than onto the remaining hulls (Fig. 3 and 4).

However this is the pressure resistance which decides on the value of total resistance and ranking sequence of the bow forms. Also, onto those forms a greater aft pressure force and – simultaneously – a smaller fore resistance acts as a rule. These conclusions are also valid for full-scale ships since in this scale the share of pressure resistance in total resistance is greater than in the case of model-scale.

○ At the water depth h = 3.4 m greater differences in hull resistance values occur than at the depth of 2.0 m (Fig.7), which means that though the resistance is smaller in the deeper water, this is the bow form which more influences the hull resistance.

○ In general, the hull and bow block coefficients constitute a rough index of quality of pushed barge hull resistance, but no unambiguous relation between those indices and hull resistance has been revealed (Fig. 6, 7, 8).

Bow block coefficient
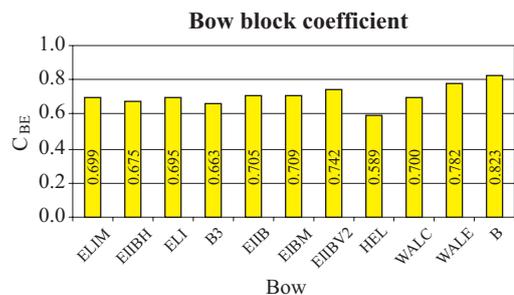
Fig. 6. The bow block coefficient C_BE (the bows are ranked on the basis of their hull resistance values at the water depth of 3.4 m, see Fig.4) .

In Fig. 7 and 8 the points are clustered in two groups. The bow forms : HEL, B, WALC and WALE belong to the first group, the remaining – to the other group. The bows of the first group have a straight, vertical or only slightly inclined stem, and greater resistance values as well. This observation suggests that the vertical or only slightly inclined stem is not favourable from the point of view of pushed barge hull resistance.
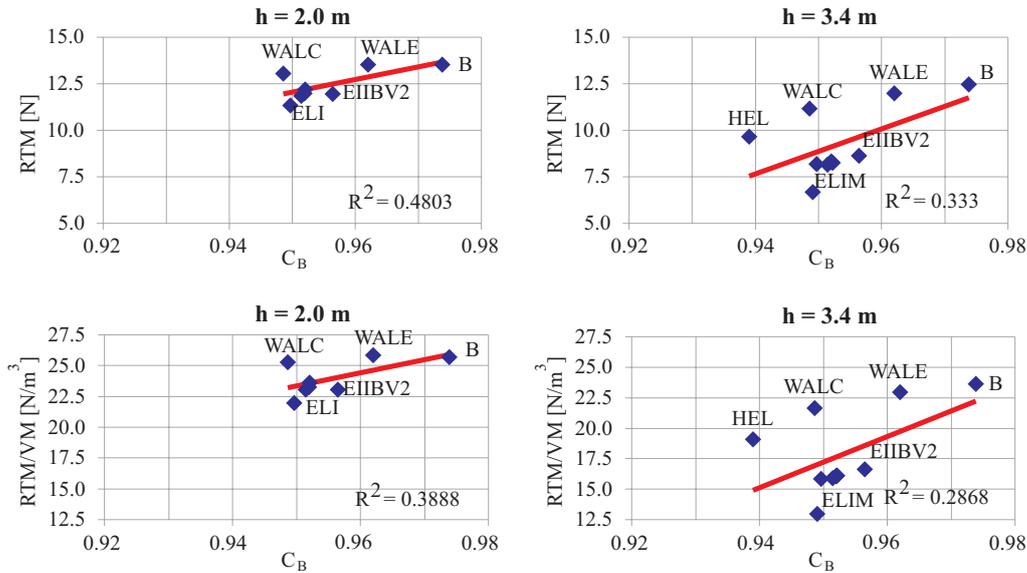
Fig. 7. *The relationship of hull resistance and the hull block coefficient C_B.*
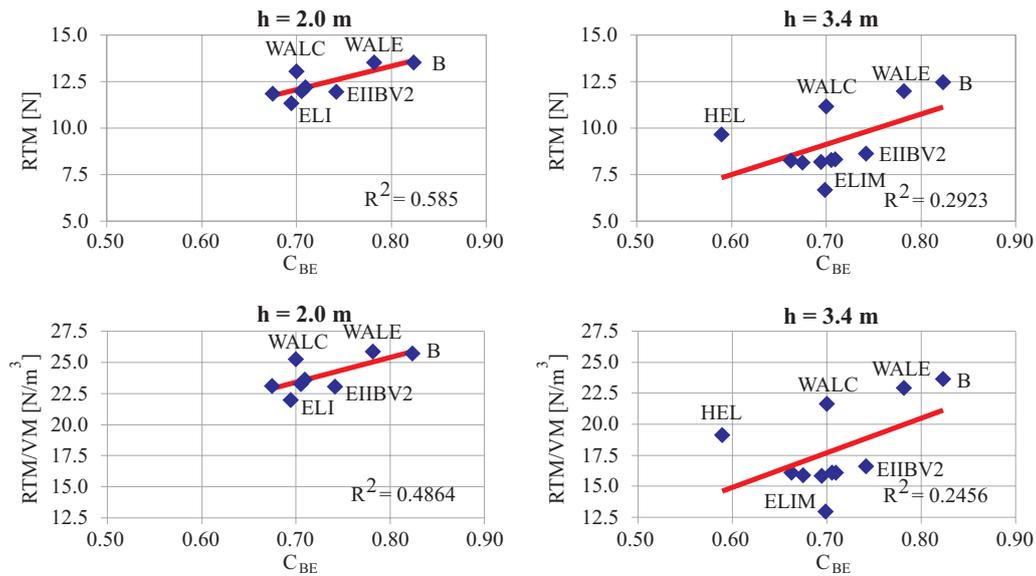
Fig. 8. *The relationship of hull resistance and the bow block coefficient C_{BE}.*

NOMENCLATURE

B	-	hull breadth
C_B	-	hull block coefficient
C_{BE}	-	bow block coefficient
Fn_h	-	Froude number ($Fn_h = V_S / \sqrt{gh}$)
g	-	gravity acceleration
h	-	water depth
L_C	-	overall length of ship
L_E	-	length of bow
T	-	design draught
V_E	-	bow volume
V_{EM}	-	bow volume in model-scale
VM	-	volume of hull underwater part in model-scale
V_S	-	ship speed
RBM	-	bow resistance in model-scale
RPM	-	pressure resistance in model-scale
RSM	-	stern resistance in model-scale
RTM	-	total resistance in model-scale
RVM	-	viscosity resistance in model-scale
RMM	-	resistance of cylindrical midship body in model-scale

BIBLIOGRAPHY

1. Kulczyk J., Tabaczek T., Werszko R., Zawiślak M., Zieliński A.: *Bow forms of inland navigation cargo vessels*. 16th International Conference on Hydrodynamics in Ship Design HYDRONAV'05. Gdańsk-Ostróda, Poland. 7-10 September 2005

2. Zawiślak, M., Tabaczek, T.: *Resistance prediction by using CFD*. Report T32-PWR-IREP-Resistance_prediction_CFD of research project INBAT within 6. Outline Program (G3RD-CT--2001-0458). August 2004

3. Zawiślak, M.: *Influence of waterway depth on pressure resistance of inland navigation ship* (in Polish). Doctoral thesis. Report of Preprint Series No. PRE 028/04, Institute of Machine Building and Operation, Wrocław University of Technology. Wrocław, 2004

4. Nussbaum, W.: *Entwicklungen der Binnenschiffsformgebung unter Berücksichtigung der Anforderungen im Flachwasserseegang*, Jahrbuch der STG, Bd 82, 1988

CONTACT WITH THE AUTHORS

Tomasz Tabaczek, D.Sc., Eng.
Prof. Jan Kulczyk
Maciej Zawiślak, D.Sc., Eng.
Institute of Machine Design and Operation,
Wrocław University of Technology
Łukasiewicza 7/9
50-371 Wrocław, POLAND
e-mail : tomasz.tabaczek@pwr.wroc.pl

Conference

HYDROACOUSTICS 2006

On 23 – 26 May 2006
at Krynica Morska upon Vistula Bay was held :

13th SYMPOSIUM ON HYDROACOUSTICS

organized by the Department of Marine Electronic Systems, Faculty of Electronics, Telecommunication and Informatics, Gdańsk University of Technology, under the auspices of : European Acoustics Association, Hydro-acoustics Section of Committee on Acoustics, Polish Academy of Sciences, and Gdańsk Division of Polish Acoustical Society.

The Symposium was commenced
by the key-note lecture on :

Research and development on underwater acoustic systems of Polish Naval University and Gdańsk University of Technology for the Polish Navy – by G. Grelowska (Polish Naval University) and L. Kilian (Gdańsk University of Technology).

During 4 plenary session of the Symposium
the following 5 invited papers were presented :

➲ *Science and technology in Polish Ministry of Defense* by W. Drąg (Polish Ministry of Defense)
➲ *New scientific multi-beam systems for fishery research applications* – by L. Nonboe (SIMRAD, Norway)
➲ *The state of the Baltic Sea hydro-acoustical investigations (selected problems)* – by Z. Klusek (Institute of Oceanology, Polish Academy of Sciences)
➲ *Synthesis and wavelet analysis of side-scan sonar sea bottom imagery* – by J. Tęgowski (Institute of Oceanology, Polish Academy of Sciences) and A. Zieliński (University of Victoria, Canada)
➲ *Quadrature phase detection in an acoustic positioning system* – by A. Zieliński (University of Victoria, Canada) and Y.Shi (Southwest Jiaotong University, China)

The remaining 25 papers were presented during 4 panel sessions. Original papers, both theoretical and experimental, concerning problems of hydro-acoustics and its applications are published in the annual journal **Hydro-acoustics**.

Miscellanea

Workshops 2006

Under this name, on 30 March ÷ 1 April 2006, Faculty of Maritime Technology, Technical University of Szczecin, arranged the series of popular scientific lectures and demonstrations to promote the courses on

Ocean Engineering and Transport

conducted at the Faculty.

Academic lecturers presented the following themes :

★ *Safety at sea* – by M. Hann
★ *Gas an oil mining from sea bed* by W. Chądzyński
★ *Contemporary maritime industry and shipping* – by T. Jastrzębski
★ *Neural networks* – by D. Pielka
★ *Shapes of sound* – by S. Weyna
★ *Super-computers and turbulence* by T. Abramowski
★ *Unconventional energy sources on ships* by W. Zeńczak
★ *Digital evolution* – by P. Nikończuk
★ *Stirling's engine* – by A. Żmuda

The last day the underwater apparatuses built at the Faculty were demonstrated. The Workshops appeared very interesting for many visitors hence it was decided to organize them every year.

Conference

SEM – ECO

On 12 May 2006 the scientific seminar on : Ecological problems in operation of combustion engines, organized by Prof. L. Piaseczny, was held at Polish Naval University.

The seminar program contained two lectures presented by the scientific workers from Warsaw University of Technology, namely :

❊ *Selected problems of emission of PM10 solid particles from exhaust gas systems of combustion engines* by M. Żegota
❊ *Development trends of combustion engines for usage vehicles* – by Z. Chłopek

Both the topics triggered very interesting discussion which enriched the knowledge passed on in the presented lectures.
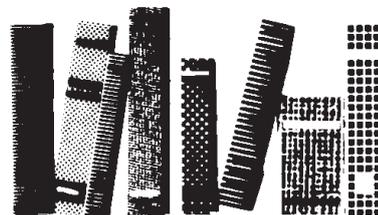
Stiffness characteristics and thermal deformations of the frame of high power marine engine

Lech Murawski
Marek Szmyt
Centrum Techniki Okrętowej S. A. (CTO)
(Ship Design and Research Centre)

ABSTRACT

In the subject-matter literature detail data on stiffness of the crankshaft foundation connected with the frame of marine main engine are still lacking. Thermal deformation models of the engine's casing, proposed by engine producers, are excessively simplified. However the parameters are crucial for the shaft-line alignment analysis as well as for the analysis of interactions between the shaft-line and engine crankshaft, especially in the case of high power engines. This paper presents a determination method of the marine engine body characteristics as well as results of example computations performed for a Sulzer 7 RTA 84 C engine installed on a ~3000 TEU container ship. It has been demonstrated that the producer's assumption about parallel displacement of the crankshaft axis in thermal working conditions is too rough. The thermal deformation of the engine is of hogging character, which results in significant change of the moment load exerted on the crankshaft and shaft line. The stiffness parameters recommended by the producers for the shaft-line alignment are estimated correctly, however they represent only engine's body flexibility, without taking into account ship's hull flexibility.

Keywords : marine main engine, main bearing, static and dynamic stiffness characteristics of bearing, thermal deformation, temperature distribution

INTRODUCTION

The aim of the presented work has been to evaluate displacements of the engine crankshaft axis in different working conditions of propulsion system [3 , 5]. In the shaft-line alignment methods the crankshaft-shaft line interaction has been considered in a simplified way so far. The crankshaft has been modelled as a linear system of cylindrical beam elements, whereas its thermal displacements and its foundation stiffness have been evaluated on the basis of simple data supplied by the producer without considering the type of the ship on which the engine has to be installed [4]. The goal of the work has been to improve representation of the boundary conditions of the marine power transmission system. It is especially important for the high power propulsion systems since in the literature many examples of the damage of the first three main bearings (counting from the driving end) of the main engine can be found [1 , 2]. One of the possible causes of such state might be the imprecise mathematical model of crankshaft, proposed for the analysis of shaft line alignment.

Within the frame of this work several analyses of the Sulzer 7 RTA 84 C engine installed on a big container ship (of ~3000 TEU capacity) were carried out. Also, the computation of engine body deformation under gravity load as well as the analysis of its thermal deformation in nominal working conditions was performed. The static stiffness (horizontal and vertical) of each of the main bearings were evaluated and then their dynamic stiffness was determined in the frequency range of 0÷30 Hz. As the forced vibration analysis was performed with the use of the modal superposition method, it was necessary to determine in advance the natural frequencies and eigenvalues in the frequency range of 0÷70 Hz. The thermal analysis requires an accurate temperature distribution on the engine body to be known. Appropriate data were obtained from comprehensive temperature measurements performed on the ship and her main engine.

ANALYSIS METHOD

The FEM model of the body of Sulzer 7 RTA 84 C engine is presented in Fig.1. Fig.2 shows a part of the model representing the engine main bearing. The engine body model contains almost 200 thousand plate and solid elements of over 930 thousand degrees of freedom**.**

The subject of the analysis was the body of Sulzer 7 RTA 84 C engine. The analysis involved, apart from heat flow, also thermal deformation and stress calculated by means of a 3D heat transfer model. The method is based on the solution of the heat flow equation (with variable coefficients). For stationary heat flow the equation has the following form:

$$\frac{\partial}{\partial x}\left[k(x, y, z)\frac{\partial T}{\partial x}\right] + \frac{\partial}{\partial y}\left[k(x, y, z)\frac{\partial T}{\partial y}\right] +$$
$$+ \frac{\partial}{\partial z}\left[k(x, y, z)\frac{\partial T}{\partial z}\right] = 0 \tag{1}$$

If the convective boundary conditions on both hot and cold surface are assumed then the following relations are valid :

$$-k(x, y, z)\frac{\partial T}{\partial y} = h(T_s - T_a) \tag{2a}$$

$$-k(x, y, z)\frac{\partial T}{\partial z} = h(T_s - T_a) \tag{2b}$$
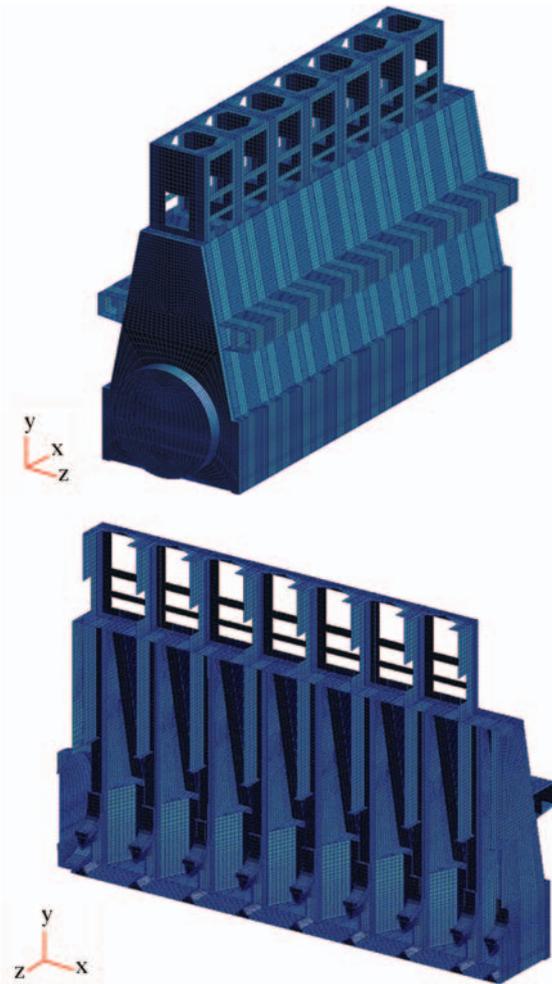
Fig. 1. FEM model of Sulzer 7 RTA 84 C engine .

Fig. 2. Main bearing frame of Sulzer 7 RTA 84 C engine .

No heat flow is assumed on other surfaces of boundary planes of the considered hull segment, which leads to the equation:

$$\frac{\partial T}{\partial x} = 0 \qquad (3)$$

The FEM thermal analysis was performed with the use of MSC NASTRAN software. MSC PATRAN software was used as a pre-and post-processor for the calculation results of the stress under thermal load.

Before starting the thermal deformation analysis of the engine it is necessary to determine temperature distribution on its body. The temperature map was created on the basis of the measurements carried out on a marine main whose size and structure was similar to those of the engine in question.

TEMPERATURE DISTRIBUTION MEASUREMENT ON ENGINE BODY

The temperature distribution measurements on the engine body were performed on the Sulzer 8 RTA 96 C engine during sea trials. The engine load was kept stable in nominal working conditions. Alfa-Tech Rytek MT 4 pyrometer was used for the measurements. The example layout of measurement points (on the port side) is shown in Fig.3. The results of measurements in those points are presented in Tab.1. On the starboard side as well as on the fore and aft end of the engine the measurement points were distributed in a similar way.
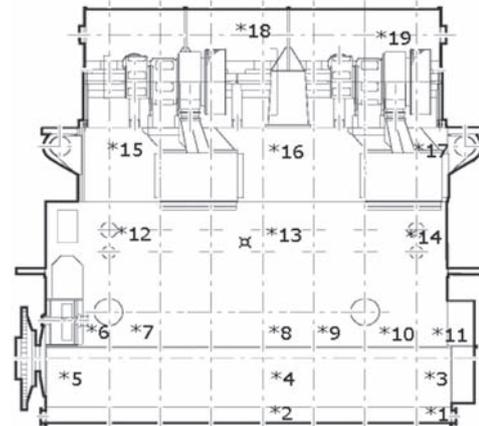
Fig. 3. Layout of the measurement points on the port side of the main engine body .

Tab. 1. Results of the temperature measurements performed on the port side of the main engine body .

Port side of the Engine					
Measure-ment point No.	Measured tempera-ture [°C]	Measure-ment point No.	Measured tempera-ture [°C]	Measure-ment point No.	Measured tempera-ture [°C]
1	37	8	52	15	51
2	44	9	49	16	50
3	52	10	52	17	57
4	53	11	49	18	60
5	54	12	50	19	63
6	49	13	54		
7	53	14	54		

THERMAL ANALYSIS OF ENGINE BODY DEFORMATION

In the numerical thermal analysis the value of heat conductivity coefficient for steel was assumed equal to 42.9 [W/m K]. The heat flow analysis was performed for the condition of the hold being hot and thermally balanced. Because of lack of more precise data the heat transfer coefficients were assumed as for heated cargo in accordance with DNV Classification Rules. The values of heat transfer coefficients are presented in Tab.2. The thermal expansion coefficient of the engine body was assumed equal to $\alpha = 1.6 \times 10^{-5}$. The temperature distribution on the engine body, shown (in °C) in Fig.4, was analogous to that obtained from the measurements.

Tab. 2. Assumed values of heat transfer coefficients [W/m² °C] .

From air in the hold to the inner bottom structure	58.1
From air in the hold to the side structure	58.1
From air in the hold to the deck structure	58.1
From outboard water to the hull shell	7400
From air to the hull shell	23.2
From air in the double bottom to the hull structure	0
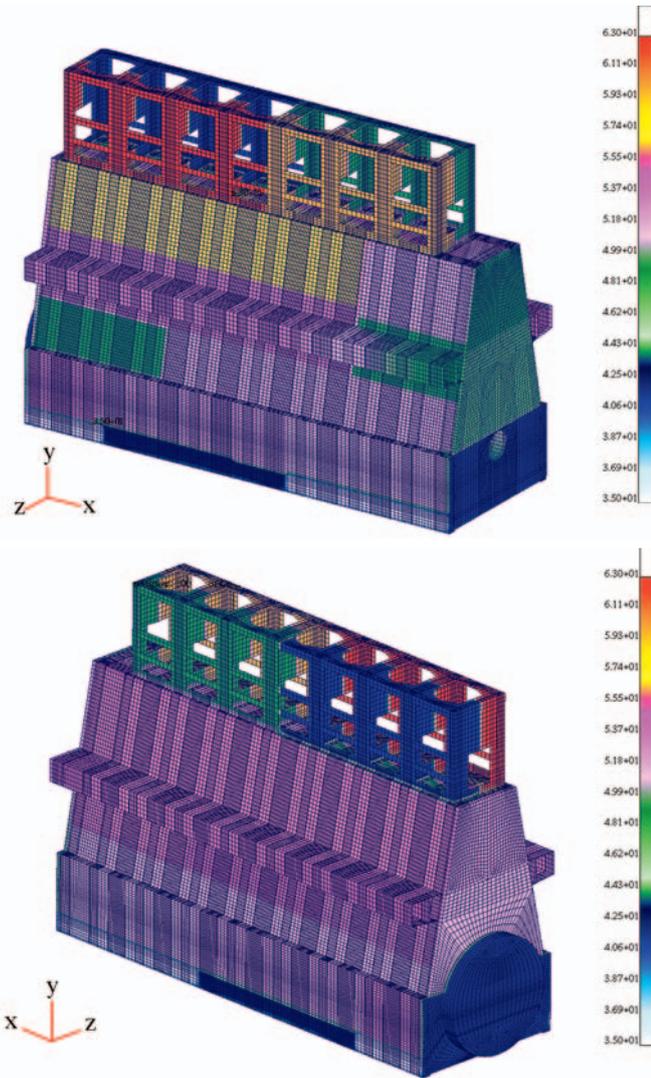
Fig. 4. Temperature distribution on the engine body, assumed for the analysis . Note : On this and all next figures the SI standard units (e.g. m, Pa) are applied .

In Fig.5 the thermal deformation of the engine body is presented in the form of fringe plot. From the point of view of the propulsion system and main engine – shaft line interaction, displacements of the engine main bearings are most important. The values of the displacements are presented in Tab.3. The bearings are numbered beginning from the driving end of the shaft line (the right-hand side of Fig.5).
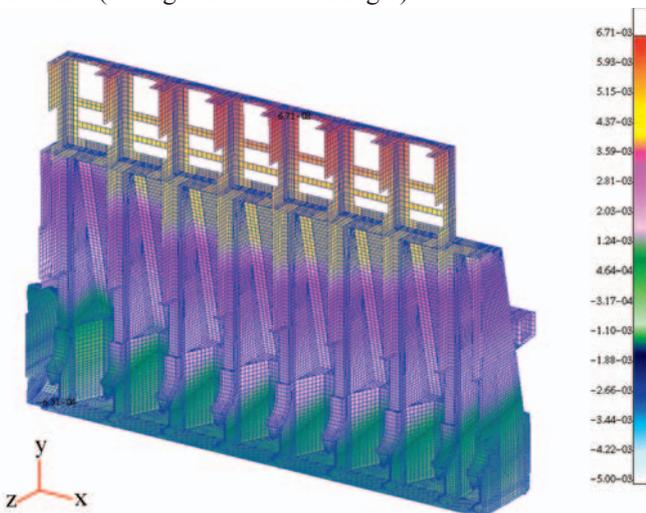
Fig. 5. Thermal deformation of the body of Sulzer 7 RTA 84 C engine .

Tab.3. Thermal displacements of the main bearings of Sulzer 7 RTA 84 C engine .

Main bearing No.	Vertical displacement [mm]	Horizontal displacement [mm]	Axial displacement [mm]
1	0.756	-0.004	1.905
2	1.086	-0.001	1.327
3	1.428	0.002	0.604
4	1.564	0.005	0.290
5	1.627	0.009	0.056
6	1.605	0.011	-0.180
7	1.498	0.010	-0.476
8	1.252	0.006	-0.948
9	0.645	-0.005	-1.986

For the crankshaft axis translation the main engine's producer recommends to use the following formula :

$$h_e = dh(T_s - T_a) \qquad (4)$$

where :

h_e – displacement of the main bearing axis [mm]
dh – thermal expansion coefficient of the engine body [mm/K]
T_s – service temperature of the engine [K]
T_a – air temperature in the engine room [K].

For the examined Sulzer 7 RTA 84 C engine the translation of the main bearing axis amounts to :

$$h_e = 18.4 \cdot 10^{-3}(53.0 - 20) = 0.607 \text{mm} \qquad (5)$$

The numerically computed value of the translation of the shaft line axis (Tab. 3) is greater than that recommended by the producer despite the fact that the measured temperature of the real engine is slightly lower than its specified service temperature. The difference for the first bearing is not particularly large (less than 20%), but other bearings are much more displaced. It seems that the producer's assumption on the parallel translation of the crankshaft axis is incorrect. The hogging deformation of the crankshaft results in a significant change of the moment transferred from the shaft line. Its effect calculated by using a precise shaft line alignment analysis would be considerable.

ANALYSIS OF STATIC STIFFNESS OF MAIN BEARINGS OF THE ENGINE

Determination of the static stiffness consists in applying unitary forces equal to mass forces and radial gas forces (of 750 kN), to each of the main bearings, one by one, first in vertical and then in horizontal direction. The achieved displacements serve to calculate the local static stiffness. The quantities are very important for shaft line alignment analysis since applying only the ship's hull stiffness may be insufficient. The main engine producers usually provide (on request) information on the crankshaft foundation stiffness but without dividing the quantity into that concerning engine body alone and ship hull. Some time ago this parameter was assumed infinitely large, now it is considered as large as 6.0×10^9 N/m. The CTO Co. gained vast experience concerning the stiffness of ship hulls of many types but no main engine body stiffness has been so far examined by this company.

The deformation of the main engine body under only gravity load was computed first. It was observed that the deformation due to gravity load was several times smaller (of the order of only 0.01mm) than that due to thermal load, cylinder mass and

gas forces. Therefore in further analysis the influence of gravity load may be neglected.

Next, was carried out the static analysis consisting in application of the load first in vertical and then in horizontal direction (18 load cases). The estimated radial forces were distributed on the main bearing surface. Tab.4 contains the static stiffness values for particular main bearings (numbered beginning from the aft – driving end of the crankshaft). The selected deformation values and stress fringe plots are presented in Fig. 6÷8.

Tab. 4. Static stiffness of the main bearings of Sulzer 7 RTA 84 C engine .

Main bearing No.	Vertical stiffness ×10⁹ [N/m]	Horizontal stiffness ×10⁹ [N/m]
1	6.615	10.942
2	6.828	11.232
3	7.317	12.229
4	7.357	12.300
5	7.364	12.325
6	7.360	12.307
7	7.329	12.248
8	7.188	12.020
9	6.312	9.689
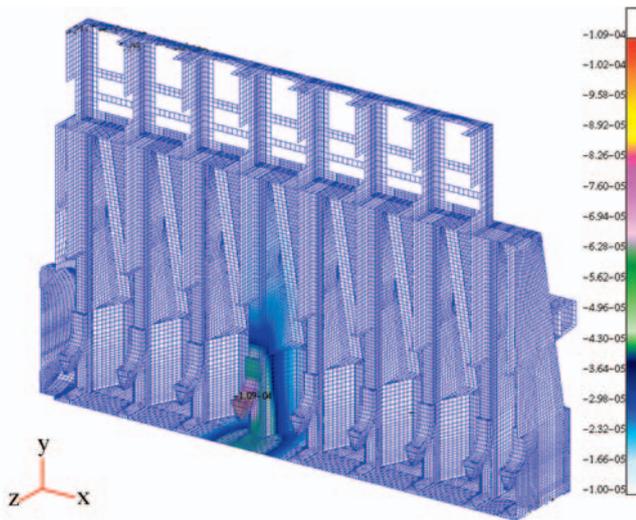
*Fig. 6. Deformation of the main engine body
under vertical load applied to 6ᵗʰ main bearing .*

*Fig. 7. Deformation of the main engine body
under horizontal load applied to 1ˢᵗ main bearing .*
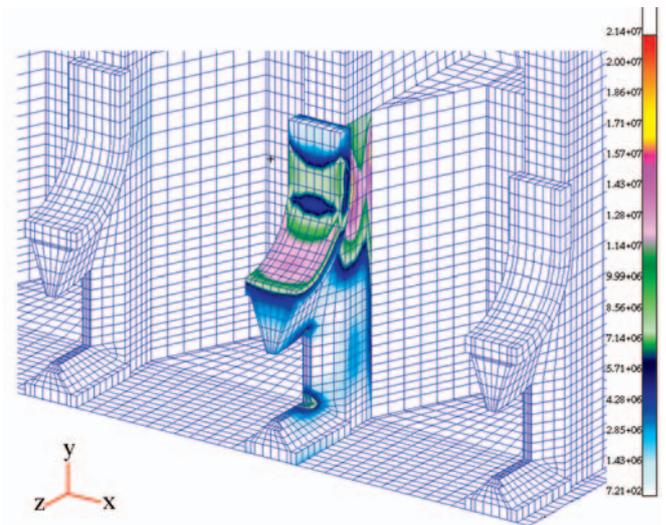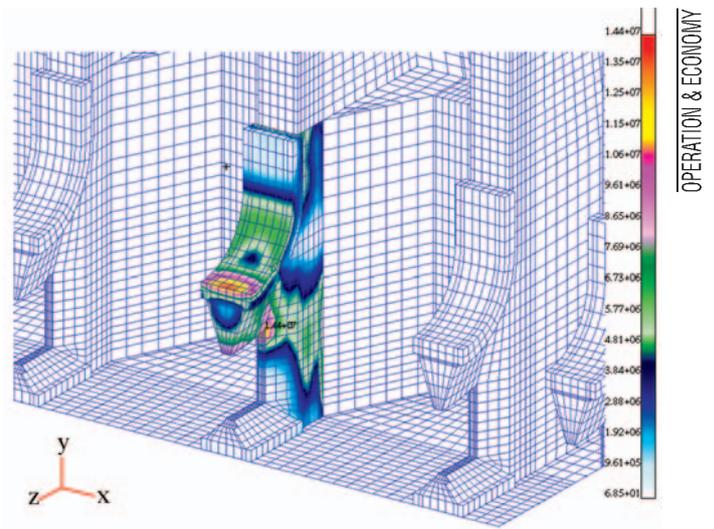
*Fig. 8. Stress in the main engine body under vertical
and horizontal load applied to 3ʳᵈ main bearing .*

On the basis of the performed analysis it can be stated that the static stiffness values specified by the producer are properly evaluated, however they represent only the flexibility of the engine body without taking into account the ship hull flexibility. In the authors' opinion in the analysis of shaft line alignment the sum of both flexibility parameters should be taken into account. It can be observed that the engine body stiffness is very high and the cylinder mass and gas forces acting on a single cylinder have a little influence on displacements of other main bearings.

It means that it is not required to take into account any coupling between particular bearings – hence there is no necessity to determine the equivalent stiffness reflecting the engine structure integrity. It is intriguing that the horizontal stiffnesses are higher than the vertical ones, not so as in the case of most other marine structures. The stress level in the main bearing structure is not high as it does not exceed 15 MPa for horizontal load and 22 MPa for vertical one.

ANALYSIS OF DYNAMIC STIFFNESS CHARACTERISTICS OF BEARINGS

The determination of the dynamic stiffness characteristics consists in applying unitary forces defined as a function of excitation frequency, to each of the main bearings, one by one, first in vertical and then in horizontal direction. The obtained displacements serve to calculate the local dynamic stiffness for

each excitation frequency, independently. These quantities are important for shaft line lateral vibration analysis. The data on the dynamic stiffness of main engine body are not available neither from literature nor from the producers.

The analysis of the dynamic stiffness of Sulzer 7 RTA 84 C engine body was carried out by using the MSC Nastran FEM solver and modal superposition method. The stiffness characteristics were determined in the frequency range of 0÷30 Hz; this way the full spectrum of possible propulsion system excitation frequencies was covered. In such case according to the authors' experience, it is recommended to calculate normal modes in the range of natural frequency, taken at least twice as wide as that. The eigenmodes were determined for frequency values up to 70 Hz. The eigenvector maps for the most important normal modes are shown in Fig. 9÷11. The applied denotation for engine body deformations, commonly used by engine producers, is as follows: **H** – lateral deformation, **X** – twisting deformation, **C** – bending deformation in vertical plane.

Fig. 11. *"C"- type normal mode at the natural frequency of 69.95 Hz .*
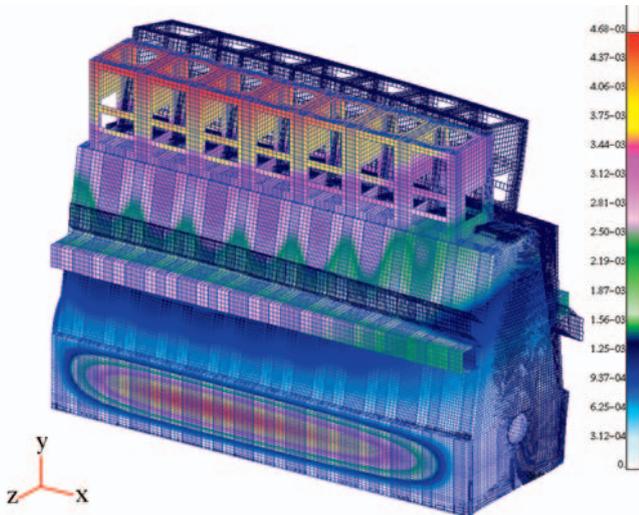
Fig. 9. *"H"- type normal mode at the natural frequency of 32.90 Hz .*
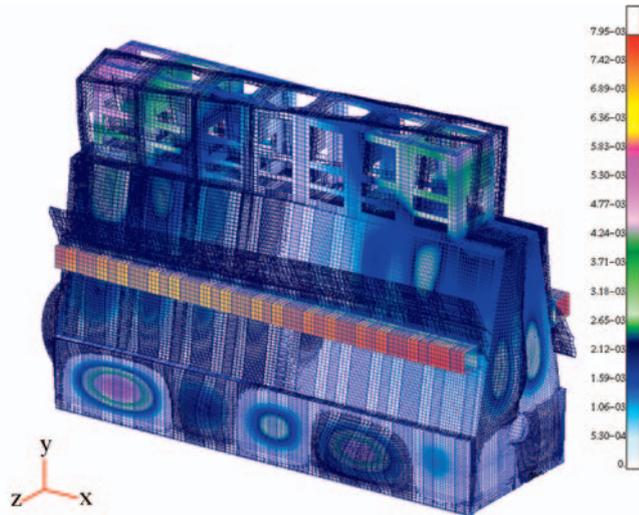
Fig. 10. *"X"- type normal mode at the natural frequency of 45.30 Hz .*

It is important that the first significant normal modes have their natural frequencies above the range of excitation frequencies of the propulsion system. And, the significant normal modes are only a few and those of interest concern the whole engine body. No significant normal modes were found in the region of the engine main bearings. It speaks well for the correct design of the engine body, i.e. of sufficiently rigid structure. In such case the resonance discontinuities of main bearing

flexibility are not expected and the characteristics appear close to linear. For this type of structure it is allowed to use only static stiffness as the expected dynamic amplification should be insignificant.

Next step was to compute forced vibration by applying first vertical load and then horizontal one to each of the engine main bearings, one by one (18 load cases). The analysis was performed within the frequency range of 0÷30 Hz. Tab.5 and 6 contain dynamic stiffness values for characteristic excitation frequencies and particular bearings (numbered beginning from the aft – driving end of the crankshaft). The nominal rotational speed of the examined engine was 100 rpm. The engine had seven cylinders, and the propeller - five blades. For such configuration the basic excitation frequencies were 8.33 Hz and 11.67 Hz.

Tab. 5. *Vertical stiffness of main bearings of Sulzer 7 RTA 84 C engine .*

Main Bearing No.	Stiffness values at 0 Hz ×10⁹ [N/m]	Stiffness values at 8.33 Hz ×10⁹ [N/m]	Stiffness values at 11.67 Hz ×10⁹ [N/m]	Stiffness values at 25 Hz ×10⁹ [N/m]
1	6.632	6.611	6.591	6.442
2	6.846	6.824	6.804	6.650
3	7.335	7.321	7.308	7.203
4	7.375	7.362	7.350	7.254
5	7.382	7.370	7.357	7.264
6	7.378	7.365	7.353	7.259
7	7.348	7.334	7.321	7.219
8	7.206	7.190	7.174	7.053
9	6.327	6.301	6.274	6.309

Tab. 6. *Horizontal stiffness of main bearings of Sulzer 7 RTA 84 C engine .*

Main bearing No.	Stiffness values at 0 Hz ×10⁹ [N/m]	Stiffness values at 8.33 Hz ×10⁹ [N/m]	Stiffness values at 11.67 Hz ×10⁹ [N/m]	Stiffness values at 25 Hz ×10⁹ [N/m]
1	10.969	10.924	10.878	10.447
2	11.260	11.208	11.155	10.616
3	12.260	12.195	12.128	11.406
4	12.331	12.266	12.199	11.444
5	12.356	12.290	12.222	11.435
6	12.338	12.271	12.201	11.388
7	12.279	12.210	12.138	11.303
8	12.050	11.974	11.895	11.010
9	9.714	9.643	9.572	8.847

The sample plots (for the main bearing No.3) of displacement of main bearing foundation in function of vertical (and subsequently horizontal) frequency are presented in Fig.12. Selected fringe plots of the engine body deformation in the region of the main bearing No. 3 for excitations in both directions are shown in Fig.13.
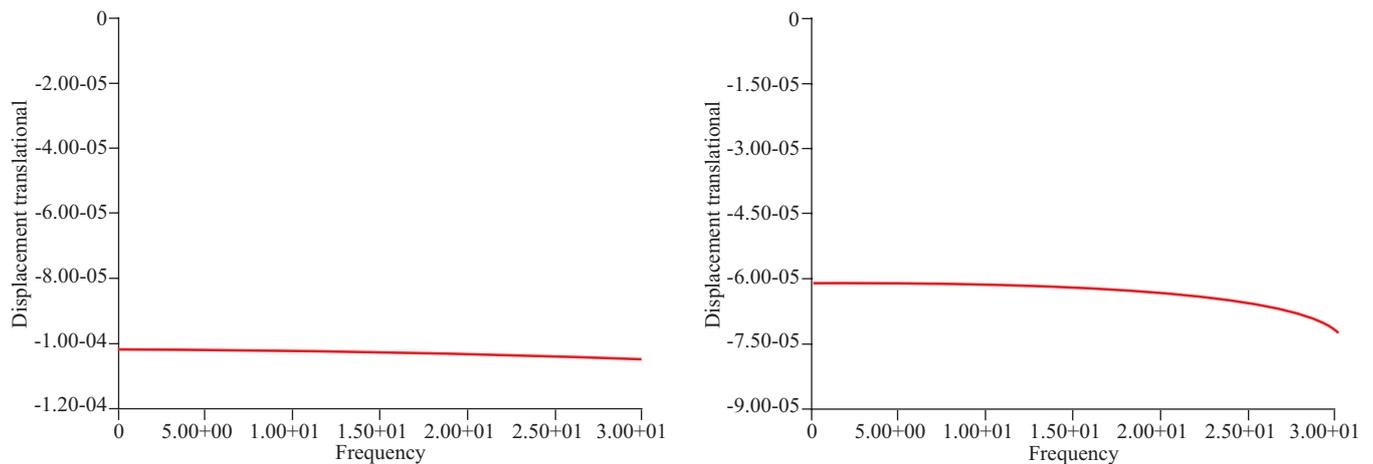
Fig. 12. Displacement of the main bearing No. 3 in function of excitation frequency .
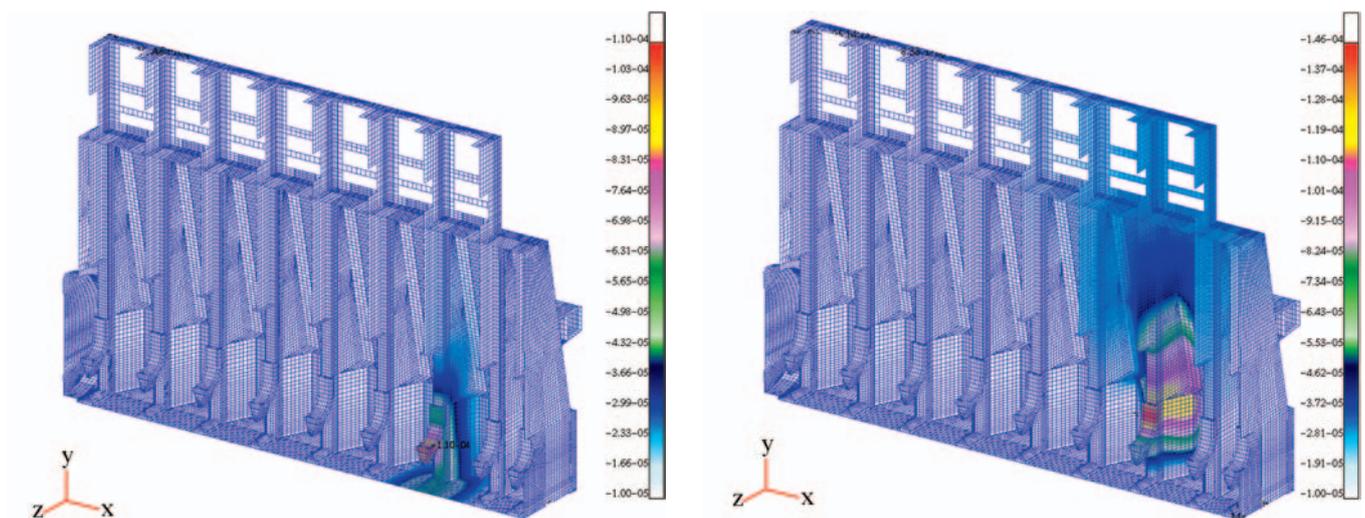
Fig. 13. Deformation of the main engine body under vertical and horizontal excitation applied to the main bearing No. 3. at the frequency of 8.33 Hz .

The dynamic stiffness values for the excitation frequency of 0 Hz are almost identical with the static stiffness (their differences are at 3rd decimal place – see Tab. 4, 5 and 6). It speaks well for the correctness of the dynamic analysis. As it was expected after performance the analysis of normal modes, the dynamic stiffness values did not significantly differ from the static ones. The stiffness decrease by 2% in vertical direction may be observed and that in horizontal direction – by less than 7%. Such change of dynamic stiffnesses can not have any significant effect on the analysis of shaft line lateral vibration. In standard (commercial) analyses the stiffness evaluation may be limited to only a static quantity which can be assumed constant in the domain of excitation frequency.

CONCLUSIONS

❍ The numerically computed shaft line displacement is greater than that recommended by the producer despite the fact that the measured temperature of the real engine is slightly lower than its specified service temperature. For the first bearing (counting from the shaft line side) the difference is not particularly big (lower than 20%), but other bearings

are much more displaced. Hence the producer's assumption on the parallel translation of the crankshaft axis seems to be incorrect. The hogging deformation of the crankshaft results in a significant change of the moment load exerted by the shaft line. It may be expected that the effect resulting from the precise shaft line alignment analysis would be considerable.

❍ On the basis of performed analysis it can be stated that the static stiffness values specified by the producer are properly evaluated, however they represent only the engine body flexibility without taking into account the ship's hull flexibility. In the shaft line alignment analysis the sum of both flexibility parameters should be taken into account. It can be observed that the engine's body stiffness is very high and the cylinder mass and gas forces acting on one cylinder have a little influence on displacements of other main bearings. Therefore it is not necessary to take into account any coupling between particular bearings.

❍ It is important that the first significant normal modes have natural frequencies above the range of excitation frequencies of the propulsion system. Moreover the significant

normal modes are few and those of interest concern the whole engine body. No significant normal modes were found in the region of the engine main bearings. It means that the engine body in question is a well-designed rigid structure. In such case the resonance discontinuities in the flexibility of main bearings should not be expected and their characteristics should be close to linear.

○ The dynamic stiffness values differ insignificantly from the static ones. The stiffness decrease by 2% can be observed in vertical direction and that by more than 7% in horizontal direction. Such change of dynamic stiffness values can not have any significant effect on results of the analysis of shaft line lateral vibration (whirling). In commercial analyses evaluation of stiffness may be limited only to determining the static value which – in the domain of excitation frequency – can be assumed constant.

○ The direction of research in question looks very promising. It would make it possible to introduce such improvements to high power propulsion systems as to avoid failures of the engine's main bearings. The presented method may be also used for more advanced and complete numerical computations carried out for main engines of other types, installed on ships having specific hulls.

○ The next step in developing the proposed method of propulsion system analysis should be incorporation of a more complex crankshaft representation based on its full 3D characteristics. The crankshaft springing effect on the shaft line alignment should be also examined.

Acknowledgements

NOMENCLATURE

dh – thermal coefficient of expansion of the engine body [mm/K]
h_e – vertical displacement of the main bearing axis [mm]
h – thermal heat transfer coefficient [W/(m^{2}K)]
k – thermal conduction coefficient [W/(mK)]
T – temperature [K]
T_a – air temperature in the engine room [K]
T_s – service temperature of the engine [K].

BIBLIOGRAPHY

1. MAN B&W Diesel A/S : *Bearings*. Copenhagen. 2000
2. MAN B&W Diesel A/S : *Elasto-hydro-dynamic evaluation of main bearing performance*. Copenhagen. 2002
3. American Bureau of Shipping: *Guidance notes on propulsion shafting alignment.* Houston. 2004
4. MAN B&W Diesel A/S : *Shafting alignment for direct coupled low-speed diesel propulsion plants.* Copenhagen. 1995
5. Wärtsilä: *Sulzer RTA-C*. Technology Review, Helsinki. 2003.

CONTACT WITH THE AUTHORS

Lech Murawski, D.Sc., M.E.
Marek Szmyt, M.Sc., M.E.
Centrum Techniki Okrętowej S. A.
Rzeczypospolitej 8
80-369 Gdańsk, POLAND
e-mail : Lech.Murawski@cto.gda.pl

Mourning

9 August 2006 was the time of a deep sorrow
for the circle of Polish shipbuilders as

Professor Jerzy Doerffer

passed away this day.

Graduate of Shipbuilding Faculty of University of Glasgow and Gdańsk University of Technology. Professor of Gdańsk University of Technology where he worked since 1948.
The organizer and the first Head of the Department of Ship Technology and its auxiliary unit.
The Dean of Shipbuilding Faculty in the years 1953-54 and 1958-64.
The Rector of Gdańsk University of Technology in the years 1964-67.

The Chairman of the Forum of Shipbuilding and Ship Repair Industry.

The creator of the scientific school in the domain of shipbuilding technology.
He was a worldwide recognized authority on this domain.

The co-author of novel design solutions and manufacturing techniques in ship technology.

Doctor *Honoris Causa* of Gdańsk University of Technology, Leningrad Shipbuilding Institute, University of Glasgow, University of Rostock, Polish Naval University and Technical University of Szczecin.

He was also honoured with William Froude Medal by the Royal Institution of Naval Architects, London.

Prof. Doerffer was not only an outstanding engineer-inventor but also a moral authority of wonderful personality. Due to his attitude and work he won respect from the side of the whole circle of Polish shipbuilders.

He was a figure-symbol of whom the circle of Polish shipbuilders boasts.

Humanist and teacher. He promoted a whole generation of Polish engineers in shipbuilding technology.

A member of prestigious scientific institutions in Poland and in the world.

Usefulness assessment of standard measuring instruments installed on sea-going ships to perform energy measurements

Zygmunt Górski,
Romuald Cwilewicz,
Gdynia Maritime University

ABSTRACT

The presented work is a contribution to discussion on usefulness of application of measurement instrumentation used on sea-going ships for energy measurement and scientific research purposes. Contemporary sea-going ships are equipped as a rule with up-to-date measurement instrumentation usually based on electronic data processing and computer technique. These authors have made many times use of such instruments in their research work. This way it was not necessary to install any special instruments, that significantly reduced measurement cost. In such cases to obtain a sufficient accuracy of measurements constitutes a crucial problem. In this paper was presented an analysis of measurement errors of some operational parameters of ship and its main propulsion system, elaborated within the frame of the KBN research project no. 9 T12D 033 17. Results of the analysis confirm usefulness of the standard measurement instrumentation installed on ships, and its sufficient accuracy.

Keywords : ship, standard measurement instrumentation, accuracy of measurements.

INTRODUCTORY COMMENTS

Contemporary sea-going ships are fitted as a rule with a rich set of control and measuring instruments. Commonly are in use analogous or digital measuring systems as well as those based on computer technique. They serve both for carrying out direct measurements and data processing in the systems for remote and programmed control of ship operation, main propulsion system and auxiliary shipboard devices.

On ships a special high-accuracy measuring instrumentation is also applied. Such instrumentation is installed only for the time of measurements and it does not belong to ship's standard equipment.

Within the frame of the KBN research project no. 9 T12D 033 17 some energy measurements were performed on the training-research ship *Horyzont II* in the period from 23.06.2001 to 14.07.2001. The measurements covered the quantities associated with operation of ship main propulsion system in various service conditions, namely main engine (ME) power output, ship speed, fuel consumption by the main propulsion system. Additionally were measured selected parameters of ME operation, interesting from the point of view of loading state of main propulsion system, e.g. exhaust gas temperature, super-charging air pressure and temperature. Also, some parameters associated with ME operation such as exhaust gas content in various loading states, were investigated. For carrying out the measurements standard measuring instruments installed on the ship as well as special measuring devices installed by the research team, were used.

The investigations were aimed among other at determination of ship propulsion characteristics. To this end the measurements of ship speed, ME power output and its fuel consumption at various rotational speeds and propeller pitch settings, were performed.

Specification of the standard measuring instruments installed on the ship and used for the research in question is as follows :

➢ for the measuring of : propeller pitch setting, rotational speed of ME and its load index – the integrated computer--based system for measuring operational parameters and control of settings of ship's main propulsion system -Wichmatic 2 Propulsion Control System, Graphic System WM 11G ECR, WM2 12G ECR, WÄRTSILÄ NSD Norway AS, having digital read-out system

➢ for the measuring of ship speed : the SAL R1 U/N 701488C electro-magnetic log of Consilium Marine Co, having digital read-out system

➢ for the measuring of : exhaust gas temperature at outlets from engine cylinders, rotational speed of turbo-blower, exhaust gas temperature before and behind the turbo-blower, supercharging air pressure and temperature, ship draught the integrated computer-based system for measuring and recording operational parameters of ship power plant devices - NORLIGHT Integrated Ship Monitoring and Control, I/O Station A 01 ER, NORIS Tachometer GMBH & Co.

➢ for the measuring of ME fuel consumption – a calibrating tank of $11 dm^3$ capacity being an element of the standard equipment of ship power plant, and a stop-watch.

By making use of the standard measuring instrumentation its usefulness had to be assessed regarding its accessibility and easiness of read-out taking, and measurement accuracy of selected parameters.

The accessibility and easiness of read-out taking is obvious. The standard measuring systems are fitted with easily readable indicators, usually in an analogue or digital form or in the form of messages displayed on a computer monitor.

In the case of investigations of such complex technical objects as ships, indication and measurement accuracy should be considered in a way different from that used in direct metrological measurements. In experimental investigations of complex objects the variability of measured quantity is assumed to be itself a basic source of errors [2]. The difference results from an influence of disturbing factors on the investigated object. Additionally, errors of the measuring method itself (including read-out errors) should by taken into consideration. In Fig.1 is shown the example distribution of measurement results within a sample, location of the mean value of the sample, as well as the range of changes resulting from variability of the object and inaccuracy of the measuring method. In the case of long-lasting measurements (e.g. of fuel consumption or a large number of repetitions) one should also analyze errors resulting e.g. from a change of service conditions during measurement taking. The whole range of values of resultant factors is called the variability measure of results [2].

The errors resulting from the above mentioned sources can be numbered among random ones. As usually assumed, they are normally distributed that makes it possible to state that in accordance with the Gauss law the average from the sample is the most probable value of the resultant factor obtained from multiple measurements :

$$\overline{z}_j = \frac{1}{r}\sum_{j=1}^{r} z_j \qquad (1)$$

where :

z_j - a single measurement result
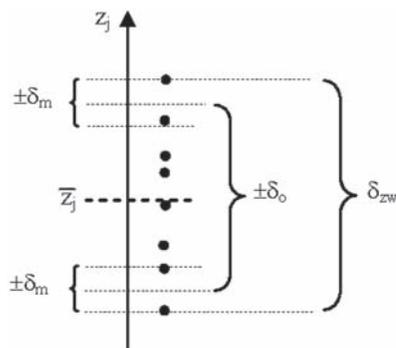r - number of repetitions of a measurement.

Fig. 1. *Diagram of position of variability measures and measurement error for an example sample of results :*
z_j *- a single measurement result, δ_m - measurement method error, δ_o - variability measure of an object, δ_{zw} - variability measure of results, $\overline{z}_j$ - average value from a sample.*

Possible systematic errors resulting from individual features of measuring instruments should be eliminated by introducing some corrections to read-out values on the basis of calibration of the measuring instruments. Also, should be rejected the results deemed to be loaded by rough errors, i.e. those significantly differing from the average from read-out values, resulting from mistakes or other hardly identifiable causes.

The basic variability measure of measurement results is their variance [2]. In the case in question, is of interest the variance

of the whole set of results coming from realization of the scope of experiment. For the same number of repetitions, r, for every point of the scope the following can be written [2, 3, 4] :

$$\sigma^2(z) = \frac{1}{m(r-1)}\sum_{u=1}^{m}\sum_{j=1}^{r}(z_j^{(u)} - \overline{z}^{(u)})^2 \qquad (2)$$

where :

m – number of measurement points
r – number of repetitions in a measurement point
$z_j^{(u)}$ – result of a single measurement
$\overline{z}^{(u)}$ – average value in a measurement point.

The root-mean-square error of results or standard deviation is equal to the square root of variance [2] :

$$\sigma(z) = \sqrt{\sigma^2(z)} = \sqrt{\frac{1}{m(r-1)}\sum_{u=1}^{m}\sum_{j=1}^{r}(z_j^{(u)} - \overline{z}^{(u)})^2} \quad (3)$$

The standard deviation of the average, i.e. the mean standard error of the average is described by means of the following expression :

$$\sigma_{\overline{z}} = \frac{\sigma(z)}{\sqrt{m\,r}} = \sqrt{\frac{1}{m^2 r(r-1)}\sum_{u=1}^{m}\sum_{j=1}^{r}(z_j^{(u)} - \overline{z}^{(u)})^2} \quad (4)$$

and the relative mean square error, i.e. the variability coefficient of results – by the expression :

$$\sigma = \frac{\sigma(z)}{\overline{z}_{\text{śr}}^{(u)}}100\% \qquad (5)$$

where :

$\overline{z}_{\text{śr}}^{(u)}$ – average from a sample of results.

In the case of the direct measurements of the independent quantities $x_1, x_2, ... x_n$, the root- mean-square error is equal to [5] :

$$\sigma(z) = \sqrt{\sigma^2(x_1) + \sigma^2(x_2) + ... + \sigma^2(x_n)} \qquad (6)$$

whereas the mean square error of the functions of direct measurements of the kind : $z = f(x_1, x_2, ... x_n)$, is equal to [5] :

$$\sigma(z) = \sqrt{\left(\frac{\delta f}{\delta(x_1)}\right)^2 \sigma^2(x_1) + \left(\frac{\delta f}{\delta(x_2)}\right)^2 \sigma^2(x_2) + ... \; ... + \left(\frac{\delta f}{\delta(x_n)}\right)^2 \sigma^2(x_n)} \qquad (7)$$

Discussion on usefulness of the standard measuring instrumentation intended for energy measurements on ships was carried out on the example of measuring the ship speed and ME fuel consumption. Accuracy of measurements and measurement method was assumed an assessing criterion.

The measurements were performed in accordance with a static, determined, multi-factor, rotational and uniform program of the technical experiment, described in [2], which contains 13 measurement points. The measurement accuracy was assessed in compliance with the above presented principle of interpretation and by using the formulae (2 ÷ 16).

ACCURACY ASSESSMENT OF SHIP SPEED MEASUREMENTS

The accuracy assessment of ship speed measurements was performed for the results obtained from two measurement series (no. 2 and 4 according to the same notation as that used in measurement reports from shipboard tests), carried out in similar sea conditions, which are presented in the table below:

No. of measurement	Ship speed v[kn]		
	Series no. 2	Series no. 4	On average
u	$v_1^{(u)} = z_1^{(u)}$	$v_2^{(u)} = z_2^{(u)}$	$\overline{v}^{(u)} = \overline{z}^{(u)}$
1	7.0	7.0	7.00
2	8.4	8.7	8.55
3	8.9	8.6	8.75
4	11.3	11.0	11.15
5	10.5	10.5	10.50
6	7.4	7.0	7.20
7	10.4	10.2	10.30
8	7.8	7.6	7.70
9	9.2	8.9	9.05
10	9.1	8.95	9.03
11	9.1	9.0	9.05
12	9.1	8.95	9.03
13	9.0	8.9	8.95
$\overline{z}_{śr}^{(u)}$			8.94

After calculations by means of the formulae (2), (3), (4) and (5) the following results were obtained :

☆ variance of measured values of ship speed $\sigma^2(v) = 0.0258$
☆ standard deviation of $\sigma(v) = 0.16$ knot
☆ standard deviation of the average value $\sigma_{\overline{z}} = 0.032$ knot
☆ variability coefficient of measured values $\sigma = 1.8\%$.

ACCURACY ASSESSMENT OF ME FUEL CONSUMPTION MEASUREMENTS

The accuracy assessment of fuel consumption measurements was performed for the results obtained in average sea conditions, presented in the table below:

No. of measurement	Fuel consumption per hour B_h [kg/h]		
	Series no. 2	Series no. 4	On average
u	$B_{h1}^{(u)} = z_1^{(u)}$	$B_{h2}^{(u)} = z_2^{(u)}$	$\overline{B}_h^{(u)} = \overline{z}^{(u)}$
1	50.22	51.84	51.03
2	75.27	83.66	79.47
3	114.13	110.13	112.13
4	183.57	182.09	182.83
5	169.91	170.36	170.14
6	52.04	55.44	53.74
7	137.25	134.85	136.05
8	74.02	74.31	74.17
9	102.33	102.43	102.43
10	101.20	101.25	101.23
11	100.27	98.91	99.59
12	101.20	101.25	101.23
13	100.91	102.32	101.65
$\overline{z}_{śr}^{(u)}$			105.05

After calculations by means of the formulae (2), (3), (4) and (5) the following results were obtained :

➢ variance of measured values of fuel consumption $\sigma^2(B_h) = 4.33$
➢ standard deviation of $\sigma(B_h) = 2.1$ kg/h
➢ standard deviation of the average value $\sigma_{\overline{z}} = 0.41$ kg/h
➢ variability coefficient of measured values $\sigma = 2.0\%$.

ACCURACY ASSESSMENT OF THE MEASUREMENT METHOD FOR SHIP SPEED

As the ship speed measurement is direct, its accuracy depends on accuracy of measuring instrument and external disturbances influencing the investigated object. The mean square error of measurement method is determined by using the relation (6). For a single measured quantity (ship speed v) it takes the form :

$$\sigma(v) = \sqrt{\sigma^2(v)} \qquad (8)$$

hence it is equal to the square root from variance of the measured values :

$$\sigma(v) = \sqrt{\frac{1}{r-1} \sum_{i=1}^{r}(v_i - \overline{v})^2} \qquad (9)$$

where :

v_i – result of a single read-out of ship speed
$\overline{v}$ – average speed in a measurement point
r – number of repetition in a measurement point.

To calculate the mean square error, were taken the measurement results at the ME rotational speed n = 830 rpm and propeller pitch H=80% for the sea conditions in centrum of measurement series 2 and 4, presented in the table below :

No.	No. of measurement series	v [kn]
1		9.2
2	2	9.1
3		9.0
4		8.9
5	4	9.0
6		8.9
On average $\overline{v}$		9.02
Number of repetitions r		6

After calculations by using the formulae (9) and (5) the following was obtained :

★ the mean square error of the ship speed measurement method $\sigma(v) = 0.12$ kn
★ variability coefficient of measurement results $\sigma = 1.3 \%$.

ACCURACY ASSESSMENT OF THE MEASUREMENT METHOD FOR ME FUEL CONSUMPTION

The ME hourly fuel consumption is the direct measurement function described by the formula :

$$B_h = \frac{3600 V \rho_t}{\tau} \qquad [kg/h] \qquad (10)$$

where :

V = 11 dm³ – volume of calibrating tank
$\rho_t = \rho_{15} - (t - 15)0.00064$ [kg/dm³] – fuel density in temperature of measurements
$\rho_{15} = 0.875$ kg/dm³ – fuel density at 15°C (standard density)

t [°C] – temperature of fuel

τ [s] – consumption time of fuel contained in calibrating tank volume.

After inserting constant values the formula takes the form :

$$B_h = \frac{35030.6 - 25.34\,t}{\tau} \quad [kg/h] \qquad (11)$$

The mean square error of the fuel consumption measurement method is calculated on the basis of the relation (7). In the case in question it is described as follows :

$$\sigma(B_h) = \sqrt{\left(\frac{\partial B_h}{\partial t}\right)^2 \sigma^2(t) + \left(\frac{\partial B_h}{\partial \tau}\right)^2 \sigma^2(\tau)} \qquad (12)$$

Values of the partial derivatives of the function (11), with respect to fuel temperature and measurement time, after inserting the average measured values (see the table below), are as follows, respectively :

$$\frac{\partial B_h}{\partial t} = \frac{-25.34}{\tau} = -0.07542 \qquad (13)$$

$$\frac{\partial B_h}{\partial \tau} = \frac{25.34\,t - 35030.6}{\tau^2} = -0.3012 \qquad (14)$$

The mean square error
of fuel temperature measurements is equal to :

$$\sigma(t) = \sqrt{\frac{1}{r-1}\sum_{i=1}^{r}(t_i - \bar{t})^2} \qquad (15)$$

where :

t_i – result of a single read-out of fuel temperature

$\bar{t}$ – average result of fuel temperature measurement

r – number of repetitions in a measurement point.

The mean square measurement error of consumption time of fuel contained in calibration tank volume is equal to :

$$\sigma(\tau) = \sqrt{\frac{1}{r-1}\sum_{i=1}^{r}(\tau_i - \bar{\tau})^2} \qquad (16)$$

where :

τ_i – result of a single read-out of consumption time of fuel contained in the calibrating tank volume

$\bar{\tau}$ – average consumption time of fuel contained in calibrating tank volume

r – number of repetitions in a measurement point.

To determine the mean square error of fuel consumption the measurement results at the ME rotational speed n = 830 rpm and propeller pitch H = 80% for the sea conditions in centrum of 2 and 4 measurement series, presented in the table below, were applied :

No.	No. of measurement series	τ		t	B_h
		min	sec	°C	kg/h
1		5	32.4	40	102.33
2	2	5	39.2	40	100.27
3		5	36.9	41	100.91
4		5	31.8	40	102.52
5	4	5	43.6	40	98.91
6		5	32.2	41	102.32
On average		5	36.0	40.3	101.21
Average time $\bar{\tau}$ [s]		336.0			
Number of repetitions r		6			

After the calculations by using the formulae (12) and (5) the following was obtained :

※ the mean square error of the fuel consumption measurement method $\sigma(B_h)$ = 1.44 kg/h

※ variability coefficient of results σ = 1.4 %.

ACCURACY ASSESSMENT OF MEASUREMENTS OF SHIP PROPELLER SHAFT TORQUE

Torque measurements were carried out with the use of special instruments installed by the measuring team. For the measurements was used the PHILIPS PR 9914/01-NC 9408499 strain-gauge torque meter with analogue read-out system.

Accuracy assessment of torque measurements was performed for the results obtained from two measurement series (no. 2 and 4 - according to the same notation as that used in the measurement reports from shipboard tests) carried out in similar conditions, presented in the table below :

No. of measurement	Torque M[Nm]		
	Series no. 2	Series no. 4	On average
u	$M_1^{(u)} = z_1^{(u)}$	$M_2^{(u)} = z_2^{(u)}$	$\overline{M}^{(u)} = \overline{z}^{(u)}$
1	3460	3332	3396
2	5895	5831	5863
3	6023	5575	5799
4	10509	10317	10413
5	8971	8715	8843
6	3845	3909	3877
7	8843	8843	8843
8	4357	4229	4293
9	6216	6216	6216
10	6248	6184	6216
11	6280	6151	6216
12	6280	6087	6184
13	6280	6023	6152
$\overline{M}_{śr}^{(u)}$			6332

After calculations by using the formulae (2), (3), (4) and (5) the following was obtained :

★ variance of measured torque values $\sigma^2(M)$ = 18003.8

★ standard deviation of $\sigma(M)$ = 134.2 Nm

★ standard deviation of the average value $\sigma_{\bar{z}}$ = 26.3 Nm

★ variability coefficient of results σ = 2.1%.

USEFULNESS ASSESSMENT OF STANDARD INSTRUMENTS FOR ENERGY MEASUREMENTS

❍ The obtained results of the assessment of measurement accuracy, performed with the use of ship standard instrumentation, are contained within the interval of 2% variability coefficient, and the assessment of accuracy of measurement methods – of 1.5%. It makes it possible to conclude that the standard measuring instruments are fully useful for carrying out energy measurements on ships.

❍ The variability coefficient of measurement results obtained by means of the special instruments for torque measuring, amounts to 2.1%, hence it is not greater than that in the case of the standard measuring instruments installed on ships.

○ the accuracy of the measurement methods, which is higher than that of measurement results, confirms that the reasoning presented in this paper is correct.

Similar energy measurements were carried out in the laboratory of combustion engines of Ship Power Plant Department, Gdynia Maritime University. As expected, the obtained results were found even more accurate in view of the stable operational conditions and loading state of the laboratory engine. For instance the variability coefficient value of measurement results of hourly fuel consumption, equal to 0.65% was obtained.

To conclude one should state that the standard measurement instrumentation which is installed as a rule onboard contemporary ships, can be successfully used for energy measurements. In particular, the measurements performed with the use of the standard instrumentation are of the following features :

⮫ a sufficient accuracy
⮫ no special instruments are required to be installed (a decrease of cost)
⮫ they can be carried out by ship's crew itself hence no additional measuring team is required (a decrease of cost)
⮫ measurement results may be used in operational and diagnostic analyses of technical state of ship's propulsion system.

NOMENCLATURE

B_h [kg/h] - hourly fuel consumption
H [%] - pitch of CP propeller (Controllable Pitch Propeller)
KBN - The State Committee for Scientific Research
M [Nm] - torque
n [rpm] - rotational speed
r - number of measurement repetitions
t [ºC] - temperature
u - number of a measurement point
v [kn] - ship speed
V [dm³] - volume
z_j - result of a single measurement
$\overline{z}_j$ - average value from a sample of measurement results
$z_j^{(u)}$ - result of a single measurement point
$z^{(u)}$ - value in a measurement point
$\overline{z}^{(u)}$ - average value in a measurement point
$\overline{z}_{śr}^{(u)}$ - average value from a sample of measurement results
δ_m - measurement method error
δ_o - variability measure of an object
δ_{zw} - variability measure of results
ρ [kg/dm³] - density
σ - relative mean square error
σ^2 - variance
$\sigma(z)$ - mean square error
σ_z - standard deviation of average value
τ [s] - time

BIBLIOGRAPHY

1. Adamkiewicz H.G.: *Statistics, applications to economy* (in Polish*)*. The Centre for Personnel Advising and Improving Co *(*Ośrodek Doradztwa i Doskonalenia Kadr Sp. z o.o.). Gdańsk. 1996
2. Polański Z.: *Planning experiments in engineering* (in Polish). State Scientific Publishing House (Państwowe Wydawnictwo Naukowe). Warszawa. 1984
3. Strzałkowski A., Śliżyński A.: *Mathematical methods for elaboration of measurement results* (in Polish), State Scientific Publishing House (Państwowe Wydawnictwo Naukowe). Warszawa. 1969
4. Szydłowski H., Kaczmarek W., Kotłowska M., Kozak A., Kudyńska J.: *Theory of measurements* (in Polish). State Scientific Publishing House (Państwowe Wydawnictwo Naukowe). Warszawa. 1981
5. Taylor J.R.: *Introduction to measurement error analysis* (in Polish). Scientific Publishing House (Państwowe Wydawnictwo Naukowe PWN). Warszawa. 1999
6. Volk W.: *Applied statistics for engineers* (in Polish). Scientific --Technical Publishers (Wydawnictwo Naukowo - Techniczne). Warszawa. 1985
7. Górski Z.: *A method to choose settings of the elements of ship main propulsion system fitted with controllable pitch propeller in the aspect of operational effectiveness of ship power plant* (in Polish). Doctoral thesis under supervision of Prof. Romuald Cwilewicz. Mechanical Faculty, Gdynia Maritime University. Gdynia. 2003

CONTACT WITH THE AUTHORS

Zygmunt Górski, D.Sc., Eng.
Assoc. Prof. Romuald Cwilewicz
Faculty of Marine Engineering,
Gdynia Maritime University
Morska 81/87
81-225 Gdynia, POLAND
e-mail : zyga@am.gdynia.pl

*C*onference

CYLINDER 2006

On 26-28 September 2006 in Zakopane, Polish town at the foot of Tatra Mountains, was held 16th country-wide technical scientific conference on :

Testing, construction, production and operation of hydraulic systems

during which were presented 28 papers whose authors and co-authors were research workers from 13 scientific research centres and 5 industrial institutions. The largest share in realization of the Conference program (6 papers) was brought in by the authors representing KOMAG, the Centre for Mechanization of Mining in Gliwice. Foreign guests from the LUBRICANT, a Czech firm, presented one paper.

Photo : Cezary Spigarski

Calculation of the mean long-term service speed of transport ship

*Continuation ot the first part of the paper published
in the Polish Maritime Research No.4(50), October 2006*

Part II
Service speed of ship sailing
on regular shipping route in real weather conditions

Tadeusz Szelangiewicz
Katarzyna Żelazny
Szczecin University of Technology

ABSTRACT

*Service speed obtainable by a ship in real weather conditions when sailing on a given shipping route, is
one of the major parameters which have great impact on ship operation costs. The so far used, very ap-
proximate method of service speed prediction based on "service margin", is very little exact. In this paper
a new method based on additional ship resistance dependent on mean statistical parameters of wave and
wind occurring on a given shipping route, is presented. The mean long-term service speed is calculated on
the basis of the calculated additional resistance and the screw propeller and propulsion engine parameters.
Also, a new definition of service margin and a way of its calculation is presented apart from the results of
the mean service speed calculation depending on ship's type and size and shipping route.*

Keywords : ship service speed, wind, waving, shipping route, service margin, long-term prediction.

SHIP PROPULSION SYSTEM

Screw propeller

Ship propulsion system is represented first of all by a propel-
ler cooperating with propulsion engine. To calculate instanta-
neous ship service speed it is necessary to know hydrodynamic
characteristics of the propeller (derived from model tests or
calculated by using approximate methods) and the characteri-
stics which describe engine load area.

In the calculations were used the characteristics of B-Wa-
geningen screw propellers [4,5], from which propeller's thrust
and torque were calculated.

Thrust of the propeller placed behind the ship hull
is expressed as follows :

$$T = \frac{R_C}{1-t} \qquad (27)$$

where :

R_C − total resistance of ship sailing in rough waters
t − thrust deduction factor.

Thrust of free propeller can be calculated from the formula :

$$T = K_T \rho_w D_p^4 n_p^2 \qquad (28)$$

where :

D_p − propeller diameter
n_p − propeller rotational speed

K_T − thrust coefficient which – for typical B-Wageningen
propellers of given values of the pitch ratio (P/D),
blade area ratio (A_E/A_0), number of blades (Z) – is
approximated by using the expression :

$$K_T = A_0 + A_1 J + A_2 J^2 + A_3 J^3 \qquad (29)$$

where :

A_0, A_1, A_2, A_3 − coefficients of the polynomial describing
thrust characteristics, depending on (P/D), (A_E/A_0), Z
J − advance coefficient :

$$J = \frac{V[1 - w(V)]}{D_p n_p} \qquad (30)$$

$w(V)$ − wake fraction depending on the ship speed V.

The propeller − when working − generates the torque Q :

$$Q = K_Q \rho_w D_p^5 n_p^2 \qquad (31)$$

where :

K_Q − torque coefficient which – like the thrust coefficient
− can be expressed for a given propeller
in the following form :

$$K_Q = B_0 + B_1 J + B_2 J^2 + B_3 J^3 \qquad (32)$$

where :

B_0, B_1, B_2, B_3 − coefficients of the polynomial describing
torque characteristics, depending on (P/D), (A_E/A_0), Z.

Free-propeller efficiency (free from ship's hull) is equal to :

$$\eta = \frac{K_T}{K_Q} \cdot \frac{J}{2\pi} \qquad (33)$$

The hydrodynamic characteristics of propeller achieved from model tests [4,5] are determined for a given Reynolds number and propeller surface state. In order to use the characteristics for the behind-the-hull propeller were introduced relevant corrections associated with influence of Reynolds number and real state of propeller surface, which makes it possible − together with knowledge of ship hull surface state − to investigate influence of ship and propeller ageing on ship service speed.

The expressions (27) and (28) for propeller thrust are valid for ship sailing in still and rough waters provided its oscillating and relative motions are so small that propeller emerging does not occur. During sailing in waves at large oscillating and relative motions the propeller operates in highly aerated water or emerges. It generates thrust variations and drop of mean effective thrust value relative to that in still water (even if the ship goes at constant speed and number of propeller rotations).

The thrust decrease is caused a.o. by an influence of water particles being in oscillating motion, on wake, as well as by propeller emerging resulting from large relative motions of the ship in waves. The thrust decrease due to ship motions in waves has been discussed in various publications where approximate formulae for estimating the influence of relative motions on operational parameters of propeller are included [3].

The propeller thrust decrease due to ship relative motions in waves is defined by means of the following coefficient [3] :

$$\beta_T = \frac{K_{Tw}\left(\dfrac{h_p}{R}\right)}{K_T} \qquad (34)$$

where :

$K_{Tw}\left(\dfrac{h_p}{R}\right)$ − thrust coefficient of emerging propeller (the quantities h_p and R are shown in Fig.11)

K_T − thrust coefficient of fully immersed propeller.

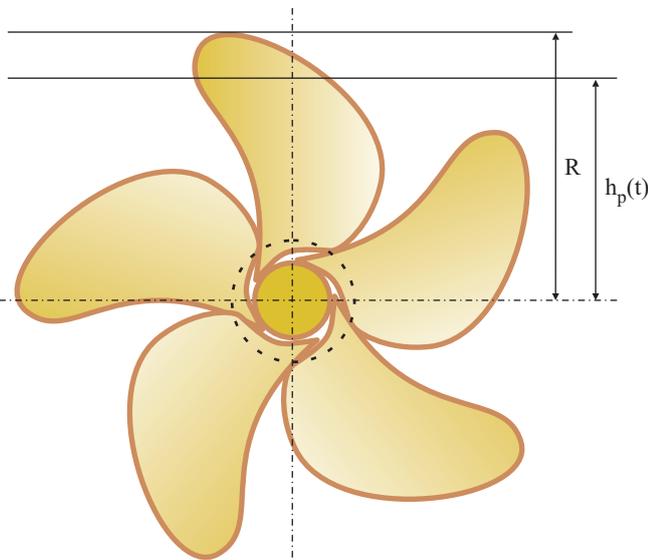Changes of values of the coefficient β_T in function of $\left(\dfrac{h_p}{R}\right)$ are shown in Fig.12, [6].

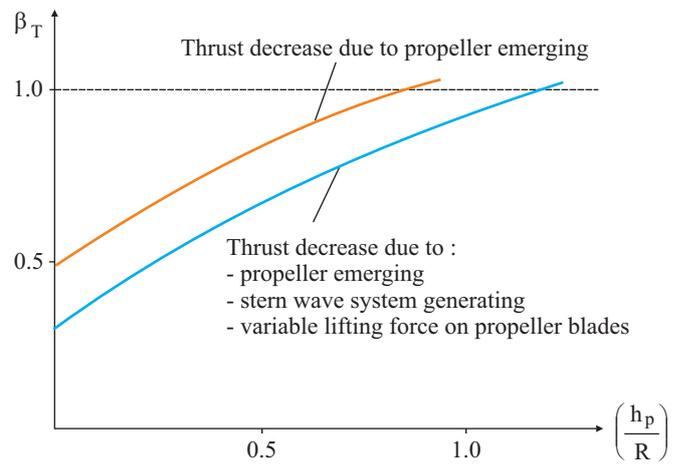*Fig. 11. The propeller draught h_p as defined in the equation (34) .*

Fig. 12. Thrust decrease during propeller emerging [6] .

In simulative propeller thrust calculations, the influence of wave parameters on propeller operation effectiveness was taken into account (detailed analysis of the phenomenon is given in [9]) whereas the propeller emergence was mitigated by intentional reduction of ship speed.

Propulsion engine

The behind-the-hull propeller loads the ship engine with its torque (31). The relation of the propeller torque and propulsion engine output power is as follows :

$$Q = \frac{P_D}{2\pi n} \qquad (35)$$

where :

P_D − power delivered to the propeller
n − rotational speed of engine (for slow-speed engines if no reduction gear is applied : $n = n_p$) :

$$P_D = N \cdot \eta_{LW} \cdot \eta_R \cdot \eta_P \qquad (36)$$

N − propulsion engine output power
η_R − relative rotative efficiency
η_{LW} − shaft-line efficiency
η_P − reduction gear efficiency, if applicable.

Engine output power for a designed ship is so selected as to obtain the propulsion system working point of the value equal to 0.85 N_n at the design (contractual) speed in still water. In real weather conditions, when wind and waves affect the ship and the additional resistance ΔR appears, then the propulsion system working point changes its location within the propulsion engine's load area. By controlling fuel charge (and this way also rotational speed of engine and propeller) the working point can be positioned in the maximum continuous rating area or the limited rating area for engine overloading (Fig.13).

Therefore, in order to find an instantaneous speed at which a given ship would sail in considered weather conditions it is necessary to know the engine load area which is constrained by relevant characteristics. This area indicates where the propulsion system working point is to be located. For instance the area of a Sulzer engine is shown in Fig.13.

The particular areas are limited by the engine performance characteristic curves in the following form :

$$N = k_m \cdot n^m \qquad (37)$$

where :

N − engine output power
k_m − coefficient for a given characteristic curve
n − engine rotational speed

m – exponent depending on a type of engine of a given producer :
  - e.g. for SULZER RTA 52, RTA 62, RT 72, RTA 84 slow speed engines it is equal to :

m = 0 – for constant rated or maximum output power
m = 1 – for constant torque characteristic curve
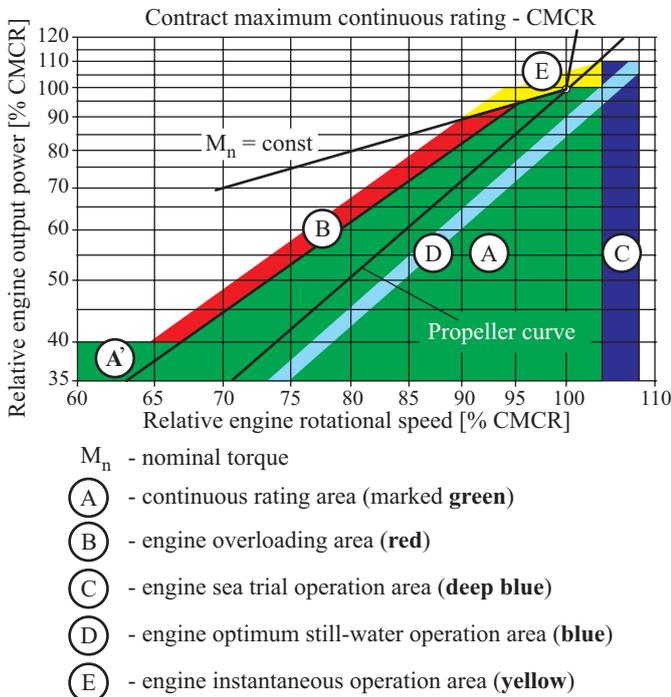m = 2.45 – for overloading characteristic curve.

Fig. 13. *The load area of an example Sulzer propulsion engine [2] .*

Service speed of ships fitted with engines of other producers can be calculated if engine characteristics limiting its load area are known.

The searching for of a working point of propulsion system and its parameters can be effected by taking into account various criteria e.g. that for maintaining a given or maximum speed, or also by using the criterion for minimum fuel consumption or maximum efficiency of whole propulsion system.

Intentional reduction of ship speed in view of hazardous wave-generated phenomena

During ship sailing in rough water ship's oscillating motions and their derivatives i.e. velocities and accelerations are the direct effect of waves. The secondary phenomena which accompany the oscillating motions are : shipping of water on deck, propeller emerging, pounding of wave to ship bottom and sides (slamming), worsening of ship stability and manoeuvrability, additional dynamic loads on hull structure. The oscillating motions and accompanying phenomena depend on parameters of ship hull and waves as well as the ship speed V and course relative to waves (the angle β_w). The phenomena, especially if very intensive, may lead directly to averages and disasters at sea. It is possible to mitigate the phenomena, e.g. ship rolling - by changing ship's course relative to waves (the angle β_w), reducing ship's speed V, or simultaneous changing ship's course and speed.

In predicting the mean service speed was made the assumption that ship's speed reduction will be performed if :

$$\overline{U}_Z > \overline{U}_{Zdop} \qquad (38)$$

where :

$\overline{U}_Z$ – mean statistical value of the wave-generated phenomenon Z considered hazardous to ship

$\overline{U}_{Zdop}$ – permissible value of the wave–generated phenomenon Z, at which the sailing ship is still safe.

In the performed calculations the ship course relative to waves was kept unchanged (though its changing is always possible), since in predicting the mean long-term ship service speed it was assumed that the ship heads the course resulting from the selected shipping route.

In assessing ship performance in waves and making decision on possible reduction of its speed, the following phenomena were taken into consideration: rolling, pitching, vertical accelerations, horizontal transverse accelerations, shipping of water on deck, slamming, propeller emerging. The calculation methods of the phenomena and the assumed acceptance criteria are presented in [1, 5, 8].

The points at which values of the parameters of ship sea-keeping qualities were calculated, are presented in Fig. 14, and in Fig.15, in the polar diagrams is shown an influence of ship speed and wave direction relative to ship on some phenomena induced by waves. The zone of unsafe intensity, i.e. where the sea-keeping criteria are exceeded , is marked red; yellow colour warns about a real hazard; green colour means the safe zone. It can be observed that reducing the speed one can mitigate intensity of the phenomena in question.
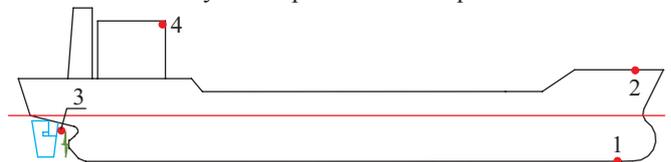
Fig. 14. *The points at which ship sea-keeping parameters were calculated : 1 – for slamming, 2 – for water shipping onto deck, and bow accelerations, 3 – for propeller emerging, 4 – for accelerations at wheelhouse.*
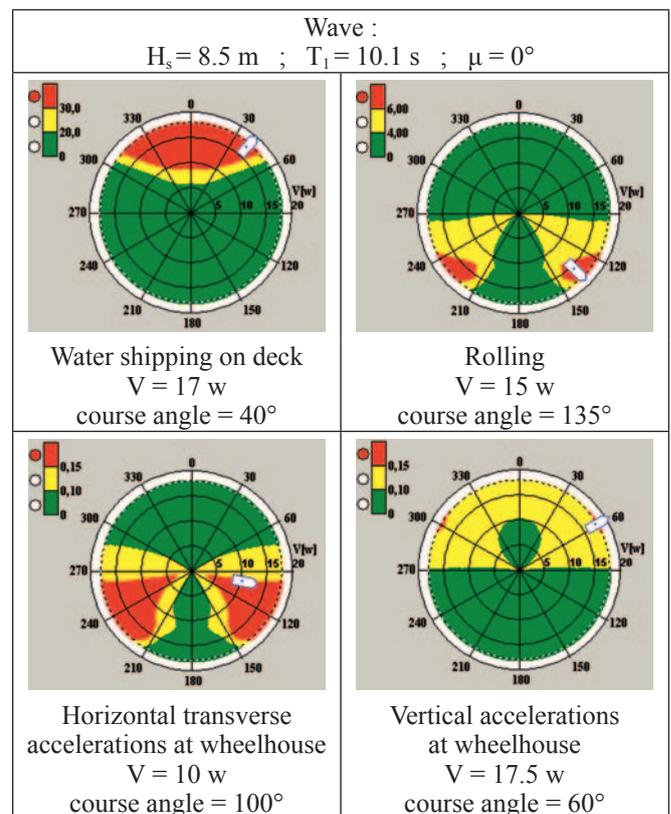
Fig. 15. *Influence course angle and speed of K1 ship on its selected sea-keeping qualities.* **Green** *- safe operation of ship.* **Yellow** *- warning on a real hazard (lower value of a relevant criterion is exceeded).* **Red** *- ship's safety is endangered (upper value of a relevant criterion is exceeded) .*

A METHOD FOR PREDICTING MEAN STATISTICAL SERVICE SPEED OF A SHIP SAILING ON A GIVEN SHIPPING ROUTE

Instantaneous service speed of ship

During ship motion in rough water, apart from still-water resistance also additional forces due to wind, waves and possible surface sea current act on the ship. These actions generate, apart from an additional resistance, a transverse force and a moment tending to rotate the ship around its vertical axis. The transverse force results in ship drifting, and the moment – in ship course changing. Ship's passive rudder is to be laid appropriately to keep ship course constant under action of the external rotating moment. Under the assumption that the ship course has to be maintained , from the solution of the following non-linear equations :

$$Y_A(V) + Y_W(V) + R_y(V,\beta) + Y_R(V,\beta,\delta_R) = 0$$
$$M_A(V) + M_W(V) + M_z(V,\beta) + M_R(V,\beta,\delta_R) = 0 \quad (39)$$

together with the relevant equations describing additional resistance forces, (presented below), for given values of the ship speed V, course angle ψ, wind parameters (V_A, γ_A), wave parameters (H_S, T, μ) and possible sea current parameters (V_C, γ_C), the following quantities can be obtained :

β −   ship drift angle
δ_R −   ship passive rudder angle
ΔR −   additional ship resistance due to wind, waves, current and passive rudder
R_C −   total ship resistance to motion.

Schematic diagram of the complete calculation algorithm of β, δ_R and R_C for given values of the ship motion parameters (V, ψ), wind parameters (V_A, γ_A), wave parameters (H_S, T, μ) and current parameters (V_C, γ_C), was presented in [9].

The instantaneous ship service speed in variable weather conditions is calculated from the solution of the set of non-linear equations in such a way as to obtain the propulsion system working point laying within the engine continuous rating zone when total ship resistance and propeller thrust , as well as propeller torque and driving engine torque become equal to each other, respectively . Making use of the equations (4), (5), (27 ÷ 36) one obtains the set of two non-linear equations :

$$(A_0 + A_1 J + A_2 J^2 + A_3 J^3)\rho_w D_p^4 n^2 - \frac{R_C}{1-t} = 0$$
$$(B_0 + B_1 J + B_2 J^2 + B_3 J^3) - \frac{N \eta_{LW} \eta_R \eta_P}{2\pi \rho_w D_p^5 n^3} = 0 \quad (40)$$

where :

J   −   advance coefficient (30)
R_C −   a function of total ship resistance, depending on the ship speed V, ship course angle ψ, wave parameters H_S, T, μ and wind parameters V_A, γ_A
N   −   driving engine output power determined by its characteristics valid within respective intervals of its rotation number n.

To solve the set of equations (40) and determine instantaneous ship service speed it is necessary to know the total ship resistance R_C which depends not only on the statistical parameters of waves and wind occurring on a given shipping route but also on current ship speed, course and drift angle. Since all the quantities depend on random parameters of waves and wind the total ship resistance should be calculated for all statistical parameters of waves and wind occurring on a given shipping route. The calculation algorithm of instantaneous ship speed is presented in [9].

Mean statistical service speed of ship sailing on a given shipping route

During the long-term sailing of ship on an assumed shipping route the additional resistance due to wave action will depend not only on a wave height (and period) but also on geographical directions: of wave, μ , and ship course , ψ. Also the additional resistance due to wind will depend, apart from the wind speed V_A, on the directions γ_A and ψ . It means that the additional resistance and also ship speed will depend on the values of the parameters of waves (H_S, T_1, μ), wind (V_A, γ_A) and ship motion (V, ψ), which may occur on a given shipping route within a long period of time.

In the case in question the surface sea current is considered to be a determinate phenomenon of the mean speed V_C and direction angle γ_C. If a ship is assumed to enter a region of large-scale surface currents then the current action will be included into ship still-water resistance.

Therefore the occurrence probability of the additional resistance ΔR of a given value, as well as the speed V which can be reached at occurrence of that additional resistance, depends on :

⊃ shipping route and probability of staying the ship in particular sea areas
⊃ the statistical parameters of waves , (H_S, T_1, μ), and wind, (V_A, γ_A), and probability of occurrence of the parameters in given sea areas
⊃ probability of occurrence of the ship motion parameters (V, ψ).

The probability of being the ship in a given situation when sailing in waves on a given route, is as follows :

$$p_w = f_A \cdot f_S \cdot f_\mu \cdot f_{HT} \cdot f_V \cdot f_\psi \quad (41)$$

where :

f_A −   probability of staying the ship in the sea area A
f_S −   probability of staying the ship in the sea area A during the season S
f_μ −   probability of occurrence of the wave direction μ in the sea area A during the season S
f_{HT} −   probability of occurrence of the wave of the parameters (H_S, T_1), propagating from the direction μ
f_V, f_ψ −   probability of the event that the ship moves with the speed V and heads the course ψ, respectively.

In a similar way can be expressed the probability p_A of being the ship in a given situation associated with wind state. In the calculations of additional resistance due to wind and waves it was assumed that wind speed and wave height are mutually correlated, hence $p_w = p_A$. As the event of being the ship in a given situation described by (41) will result in generating an additional resistance and achieving a determined speed, hence :

$$p_w = p_R = p_V \quad (42)$$

where :

p_R −   partial occurrence probability (in given conditions) of additional resistance
p_V −   partial occurrence probability (in given conditions) of instantaneous ship service speed.

Values of the additional resistance due to wind, R_{XA}, and that due to waves, R_{XW}, depend on random parameters of wind

and waves. Therefore the same values of R_{XA} and R_{XW} can occur for different values of the parameters V_A, γ_A, H_S, T_1, μ, V, ψ. For each of the values of this way calculated additional resistance, a value of ship speed is calculated (the criteria concerning sea-keeping qualities are simultaneously examined to execute possible speed reduction in order not to violate them at given wave and wind conditions).

The total probability P_{TV} of achieving the ship speed V at a given value of the additional resistance ΔR, is as follows :

$$P_{TV} = \sum_{A=1}^{n_A}\sum_{S=1}^{n_S}\sum_{\mu=1}^{n_\mu}\sum_{H,T=1}^{n_{HT}}\sum_{V=1}^{n_V}\sum_{\psi=1}^{n_\psi} P_{Vi}[V_i(\Delta R_i)] \qquad (43)$$

where :

$V_i(\Delta R_i)$ – instantaneous ship service speed in function of instantaneous additional ship resistance

n_A, n_S, n_μ, n_{HT}, n_V, n_ψ – numbers of sea areas (crossed by a given ship), seasons, wave directions, wave parameters, ship speeds and courses, respectively.

By calculating the distribution function of occurrence probability, $f(V_i)$, of the instantaneous ship speed V_i the mean long-term ship service speed for a given shipping route, can be determined as follows :

$$\overline{V_E} = \frac{\displaystyle\sum_{i=1}^{n_V} P_{TV_i} V_i(\Delta R = const)}{\displaystyle\sum_{i=1}^{n_V} P_{TV_i}} \qquad (44)$$

where :

n_V – number of intervals containing similar values of the instantaneous ship service speeds.

On the basis of the presented calculation formula for the mean ship service speed, (44), were performed relevant calculations and analyses for example ships and shipping routes, whose results will be presented in the 3rd part of the paper.

NOMENCLATURE

$\left(\dfrac{A_E}{A_0}\right)$ – propeller blade area ratio

A_0, A_1, A_2, A_3 – coefficients of the polynomial describing thrust characteristics

B_0, B_1, B_2, B_3 – coefficients of the polynomial describing torque characteristics

D_p – propeller diameter

f_A – probability of staying the ship in the sea area A

f_{HT} – probability of occurrence of the wave of the parameters (H_S, T_1), propagating from the direction μ

f_S – probability of staying the ship in the sea area A during the season S

f_V, f_ψ – probability of the event that the ship moves with the speed V and heads the course ψ, respectively

$f_{\gamma A}$ – probability of occurrence of a given wind direction

H_S – significant wave height

J – advance coefficient

K_T – thrust coefficient

K_{Tw} – thrust coefficient of emerging propeller

K_Q – torque coefficient

k_m – coefficient of a given characteristic curve of engine performance

N – propulsion engine output power

N_n – nominal output power of propulsion engine

n – rotational speed of engine

n_n – nominal rotational speed of engine

n_p – rotational speed of propeller

$\left(\dfrac{P}{D}\right)$ – propeller pitch ratio

P_D – power delivered to propeller

P_{TV} – combined probability of reaching a given value of instantaneous ship service speed at occurrence of a given value of instantaneous additional ship resistance

p_w – partial probability of staying the ship in a given situation

p_R – partial occurrence probability of instantaneous additional resistance (in given conditions)

p_v – partial occurrence probability of instantaneous ship service speed (in given conditions)

Q – propeller torque

R_C – total ship resistance to motion

R_{xA}, R_{yA}, M_{zA} – mean wind-induced forces exerted to going ship (R_{xA} - additional ship resistance due to wind)

R_{xR}, R_{yR}, M_{zR} – passive rudder forces (R_{xR} - additional ship resistance due to rudder)

R_{xW}, R_{yW}, M_{zW} – mean wave-induced drift forces (R_{xW} - additional ship resistance due to waves)

T – free-propeller thrust

T_1 – mean characteristic wave period

t – thrust deduction factor

U_z – mean statistical value of the wave-induced phenomenon Z

V – ship speed

V_A – wind speed

V_C – sea current speed

$\overline{V_E}$ – mean statistical ship service speed

w – wake fraction

Z – number of propeller blades

β – ship drift angle

β_T – coefficient of propeller thrust decrease

γ_A – geographical direction of wind

γ_C – geographical direction of sea current

ΔR – additional ship resistance due to weather conditions

δ_R – passive rudder angle

η_0 – free-propeller efficiency

η_P – reduction gear efficiency

η_R – propeller rotative efficiency

η_{LW} – shaft-line efficiency

λ – rudder aspect ratio

μ – geographical direction of wave

ρ_w – water density

ψ – geographical direction of ship course

BIBLIOGRAPHY

1. Dudziak J.: *Theory of ship* (in Polish). Maritime Publishing House (Wydawnictwo Morskie), Gdańsk, 1988

2. SULZER : General Technical Data for Marine Diesel Engines, 1986

3. Holtrop J.: *A Statistical Re-analysis of Resistance and Propulsion Data*. International Shipbuilding Progress, No. 363, 1984

4. Holtrop J., Mennen G.G.J.: *An Approximate Power Prediction Method*. International Shipbuilding Progress, Vol. 29, No. 335, 1982

5. Karppinen T.: *Criteria for Sea-keeping Performance Predictions*. Technical Research Centre of Finland, Ship Laboratory, ESPOO, Helsingfors, 1987

6. Minsaas K.J., Thon H.J., Kauczyński W.: *Influence of Ocean Environment on Thruster Performance*. Proc. of. Int. Symp. Propeller and Cavitation, Supplementary volume. Shanghai 1986. The Editorial Office of Shipbuilding of China

7. Oosterveld M.W.C., van Oossanen P.: *Further Computer-Analyzed Data for the Wageningen B-Screw Series*. International Shipbuilding Progress, Vol. 22, No. 251/1975

8. Szelangiewicz T.: *Ship's operational effectiveness factor as criterion of cargo ship design estimation*. Marine Technology Transactions. Polish Academy of Sciences, Branch in Gdańsk. Vol. 11/2000

9. Żelazny K.: *Numerical prediction of mean long-term service speed of transport ship* (in Polish). Doctoral thesis. Faculty of Maritime Technology , Szczecin University of Technology. 2005.